# 18

# Modelling Biological Interactions in Aquatic Sediments as Coupled Reactive Transport

Filip J. R. Meysman, Oleksiy S. Galaktionov, Stephane Madani, and Jack J. Middelburg

## Abstract

Biogeochemical processes in surface sediments are characterized by a reciprocal coupling between macrofauna, microbiology, and geochemistry. Up to present, reactive-transport models have been mainly implemented from a geochemical perspective, so-called early diagenetic models. In this chapter, we evaluate the possibilities and limitations of such diagenetic models as ecological tools, i.e. to assess the interactions between microbial and macrofaunal components. Despite the strong biological abstraction, diagenetic models can be considered as rudimentary ecosystems models, because the metabolism of bacteria and the activity of macrofauna is implicitly modelled. Effectively, present models incorporate microbial competition for metabolic resources (organic matter [OM], terminal electron acceptors) and the effect that macrofauna exerts on this competition via the redistribution of solute and solid reactants.

To illustrate these interactions, a highly idealized sediment ecosystem model is constructed, incorporating five functional groups, i.e. three microorganisms (oxic respirers, sulphate reducers, sulphide oxidizers) and two macroorganisms (small bioturbators and large bioirrigators). The model predicts the steady-state values for a number of biogeochemical variables (so-called ecosystem functions) for a load of OM that varies from deep-sea to nearshore conditions. We performed a sensitivity analysis for the biological parameters in the model and compared numerical results with theoretical first-order approximations. Despite the high level of abstraction, we show that the model captures some important features of the benthic ecosystem. We conclude that the present reactive-transport formalism could serve as a basic platform for developing more advanced benthic ecosystem models. Future extensions could include (1) the feedback of microbial metabolism on macrofaunal activity via the environment, (2) the incorporation of biomass dynamics of bacteria and macrofauna, and (3) the inclusion of direct interactions between biological components.

## Introduction: Where Is the Biology in Early Diagenetic Models?

Quantitative studies of surface sediments (the top 0–50 cm of oceans, estuaries, lakes, and rivers) are typically based upon the application of so-called general diagenetic models

Macro- and Microorganisms in Marine Sediments
Coastal and Estuarine Studies 60

10.1029/60CE19



Publ. 3361 Netherlands Institute of Ecology (NIOO-KNAW)

(Berner, 1980; Boudreau, 1997), which provide an integrated reactive-transport description of aquatic sediments. Over the past four decades the field has shifted from simple analytic models to large and complex numerical models, which aim at a realistic prediction and mechanistic description of sediment biogeochemistry (Soetaert et al., 1996a; Boudreau, 1996a; Van Cappellen and Wang, 1996; Hensen et al., 1997; Wijsman et al., 2002; Berg et al., 2003; Meysman et al., 2003b). Early diagenetic modelling theory is closely related to "subsurface" reactive-transport fields, such as groundwater geochemistry, contaminant hydrology, mineral–rock interactions, and petroleum engineering (Huyakorn and Pinder, 1983; Lichtner, 1985; Bear and Bachmat, 1991; Steefel and MacQuarrie, 1996). Common to these disciplines is the description of the sediment as a two-phase porous medium, consisting of both the porewater and the solid-phase sediment grains. Yet, substantial differences exist with regard to the inclusion and description of biological activity.

Surface sediments receive an input of fresh OM and oxygen from the overlying water column. These two factors are the driving force for intense microbial processing, but they also enable the presence of a diverse community of eukaryotic organisms, ranging in size from microfauna (<63 μm), over meiofauna (63 μm–1 mm) to macrofauna (>1 mm). Consequently, reactive-transport models of surface sediments need to deal with the presence of these biological components. Effectively, these organisms display their own specific modes of transport (i.e. movement) and reaction (i.e. metabolism), different from those of the porewater and the solid phase. So, rather than considering the sediment environment a mere two-phase system, one might—at least in principle—extend the model description with additional and separate "organism" phases (Meysman, 2001).

However, this is not the way organisms are treated in the current reactive-transport models of aquatic sediments. At first sight, one might consider it a surprising, if not amusing, twist of fate to find a chapter on reactive-transport modelling in a book on the interactions between micro- and macroorganisms. The reason for this wonder is the strong abstraction of biological processes in the current model formulation of early diagenesis (Meysman, 2001; Soetaert et al., 2002). Up to the present, neither microorganisms nor macrofauna have been given a true "material" representation in such models. By this we mean that biomass is not incorporated as a true state variable, and hence the population dynamics of neither bacteria nor macrofauna is modelled. In essence, one can state that both bacteria and macrofauna function as "ghosts" within the present models, i.e. as agents that perpetrate a certain effect without being physically present.

Macrofauna is considered an important "transport agent" for both solids and solutes in surface sediments (e.g. Rhoads, 1974; Aller, 1982, 2001); consequently, early diagenetic models typically include bioturbation (solid transport) and bioirrigation (solute transport) in addition to physical transport (Berner, 1980; Boudreau, 1997; Meysman, 2001). The presence of such biologically induced transport constitutes the main distinction between reactive-transport models of surface and subsurface environments. In particular, in models of groundwater geochemistry and mineral–rock interactions, the solid matrix is assumed immobile and transport acts only on dissolved species (Bear and Bachmat, 1991; Steefel and MacQuarrie, 1996). Two remarkable aspects further typify the inclusion of macrofauna in diagenetic models. Firstly, bioturbation and bioirrigation terms are not dependent on the density or biomass of the macrofauna that actually perpetuate the transport. To the authors' knowledge, diagenetic models have not yet included macrofaunal biomass dynamics. Consequently, macrofauna biology is present only in the form of transport parameters, which typically remain constant with time, implying the strong assumption that biological activity remains constant in time. A second striking simplification is that macrofauna display no metabolism in early diagenetic models. The classical scheme of OM decomposition envisions six metabolic pathways (aerobic respiration, denitrification, manganese oxide reduction, iron hydroxide reduction, sulphate reduction, methanogenesis) where

different species or consortia of bacteria employ distinctly different terminal electron acceptors (Fenchel and Blackburn, 1998). In this view, all OM mineralization is implicitly attributed to microbial activity. De facto, macrofauna inexorably mix porewater and sediment particles, without needing to obtain catabolic energy from feeding. Mischievously, one could say that diagenetic models represent macrofauna not only as ghosts but also as perpetuum mobiles.

In contrast to macrofauna, bacteria are considered to be "reactive agents" that catalyze chemical transformations associated with microbial metabolism (see Hunter et al., 1998, for an overview of how microbial activity influences chemical dynamics in sediment environments). As with macrofauna, early diagenetic models generally do not account for microbial biomass dynamics (except Talin et al., 2003). So, as for a true chemical catalyst, the kinetic rate expression describing microbial reactions is typically not dependent on microbial biomass (Boudreau, 1992; Boudreau, this volume). In this respect, early diagenesis differs from the terrestrial soil sciences and subsurface hydrogeochemistry, where models often include an explicit reactive-transport equation for microbial biomass (e.g. Rittman and VanBriesen, 1996; Wang and Papenguth, 2001; Brun and Engesgaard, 2003; Barry et al., 2004). Generally, the bacterial biomass equation in these models includes only reactive terms, i.e. bacterial growth and decay terms (e.g. Salvage and Yeh, 1998; Brun and Engesgaard, 2003), although in few cases, bacterial transport has been modelled (e.g. Tan and Bond, 1996).

## Early Diagenetic Models as Geochemical Tools

In summary, early diagenetic models consider macrofauna as "transport agents" without reactive metabolism, while conversely, bacteria are modelled as pure "reactive catalysts" that are not subject to autonomous transport. This crude description of biology has to a large extent historical roots, as early diagenetic modelling theory was originally conceived to answer "pure" geochemical questions (Goldberg and Koide, 1962; Berner, 1964). In fact, most present-day diagenetic models are still focused on geochemical issues, i.e. elemental cycling, an accurate prediction of concentration profiles, and a proper estimation of reaction rates (Soetaert et al., 1996a; Boudreau, 1996a; Van Cappellen and Wang, 1996; Hensen et al., 1997; Wijsman et al., 2002; Berg et al., 2003; Meysman et al., 2003b). Although microbial metabolism and macrofaunal mixing were readily recognized as indispensable for an appropriate description of surface-sediment geochemistry (e.g. Goldberg and Koide, 1962; Rhoads, 1974; Aller, 1980), one has chosen to represent these biological effects in a most parsimonious way. The underlying idea is that early diagenetic models should accurately represent the influence of biology on geochemistry, but one is not interested in an accurate representation of the biology as such.

From a geochemical viewpoint, and given the questions addressed in early diagenesis, the strong abstraction of biology may be in fact justifiable. (1) *The absence of macrofauna metabolism.* Although data are scarce and show quite some temporal and spatial variability, an average value of 15–20% has been put forward for the contribution of macrofauna respiration to the total OM mineralization (Herman et al., 1999). Roughly half of this macrofaunal respiration is due to suspension feeders and surface-deposit feeders, which process OM that does not actually enter the sediment. Accordingly, at least 90% of the sediment mineralization may be attributed to bacteria. So, the neglect of macrofaunal metabolism seems appropriate in a first-order approach. (2) *The absence of microbial biomass dynamics.* Steady-state models of OM diagenesis have intrinsically a long time scale (10–100 years), which is associated with relatively slow burial, bioturbation, and mineralization of OM. Conversely, the characteristic time scale of microbial biomass dynamics is typically much shorter (days up to weeks for slowly growing species such as nitrifiers). Accordingly,

bacterial biomass can be justifiably considered in a quasi-steady state with respect to gradual biogeochemical changes associated with OM processing (Boudreau, 1999; Wang and Papenguth, 2001). Both experimental data (Westrich and Berner, 1984) and theoretical modelling (Boudreau, 1992) support the independence of OM mineralization rates from microbial biomass on longer time scales (see also discussion by Boudreau, this volume). (3) *The absence of macrofaunal biomass dynamics*. Compared with bacteria, the biomass dynamics of the macrofauna are slower and show clear seasonal fluctuations in biomass and activity (Herman et al., 1999). However, given the long time scale associated with OM decomposition, the bioturbation and bioirrigation coefficients in the model should only reflect yearly averages in macrofaunal activity. Therefore, for a given OM flux to the sediment (i.e. a constant supply of food), it is reasonable to assume a stable year-averaged macrofauna community with a constant bioturbation and bioirrigation activity (Soetaert et al., 1996b).

## Early Diagenetic Models as Ecosystem Models

Clearly, early diagenetic models differ from benthic ecosystem models in focus and approach (Meysman, 2001; Soetaert et al., 2002). The former merge a sophisticated description of the geochemical environment, i.e. a spatially explicit description via partial differential equations, with a most economical description of biological actors. In contrast, benthic ecosystem models typically incorporate complex biology, i.e. the biomass dynamics of various functional groups of organisms. At the same time, these models are typically restricted to a very rudimentary description of the geochemical context, i.e. one type of OM termed "detritus" (Moore et al., 2004) and a box-model description without spatial gradients (e.g. Pace et al., 1982; Chardy and Dauvin, 1992; Ebenhoh et al., 1995; Blackford, 1997). However, the diversity and functioning of the microbial community is linked to small-scale geochemical gradients ($O_2$, $H_2S$, organic C) within the sediment. Therefore, a proper inclusion of the microbial compartment requires a spatially explicit description of the sediment.

An intriguing question in this respect is to what extent (spatially explicit) early diagenetic models can be used to study the interactions between micro- and macroorganisms? In other words, what ecological conclusions—if any—could be drawn from the output of an early diagenetic model when used as a simplified ecosystem model? Given the biological simplicity exhibited by early diagenetic models as documented above, one is inclined to be skeptical, especially due to the absence of any *direct interactions* (grazing of bacteria by macrofauna, viral lysis, predation on macrofauna by larger epibenthic fauna). However, diagenetic models do provide a detailed biogeochemical description of the sediment environment, and as a consequence, they offer—at least in theory—a suitable way to investigate *indirect interactions*, i.e. those interactions that run via the environment, e.g. competition for metabolic resources (OM, terminal electron acceptors) or inhibition by the release of toxic metabolites ($H_2S$).

Given this restriction to indirect interactions, a diagenetic model *can* be interpreted as an idealized sediment ecosystem model if one links the biological parameters in the diagenetic model to so-called "model organisms". Effectively, each "model organism" represents a functional group of organisms that perpetrates a certain biogeochemical process. Microorganisms are represented by a specific chemical reaction, macroorganisms are represented by a specific transport process. In this view, diagenetic models effectively describe the activity of model organisms, though not their biomass, as is the case in ecological models. As a consequence, the "success" of a given model organism is measured by its activity, i.e. the reaction rate in the case of microorganisms and the transport rate in the case of macrofauna. This activity is then modulated by the geochemical composition of the environment (e.g. via ambient concentrations of OM, $O_2$, $H_2S$). Consequently, when other model organisms alter the geochemical state of the environment, they will influence the success of the organism.

For microorganisms, such modulation is clear from the presence of the concentrations of OM and terminal electron acceptors in the kinetic rates expressions of microbially catalyzed reactions. However, the modulation of macrofaunal transport coefficients (i.e. bioturbation and bioirrigation coefficients) is usually not incorporated in the standard diagenetic model description. In other words, macrofauna is allowed to influence the microbiology, but not the other way round. We are aware of only a few studies where macrofaunal activity has been made dependent on the geochemical composition of the sediment. Dhakar and Burdige (1996) employed a bioturbation coefficient that was dependent on the average oxygen concentration. Boudreau (1998) advanced the resource-feedback model for bioturbation, where bacteria determine the distribution of OM, which in turn determines the food density and the bioturbation activity of macrofauna. Herman et al. (1999) and Dauwe et al. (2001) used a similar resource feedback for bioturbation to investigate the competition between for OM between macrofauna and bacteria as a function of depth in the sediment.

## Modelling Strategy

To establish a closer linkage between ecology and geochemistry, we would like to investigate the potential of reactive-transport models for the assessment of indirect interactions between benthic organisms that run via the environment, i.e. interactions that are modulated by the geochemical state of the sediment. From the introduction, it is clear that such an enterprise is at the edge of the present modelling expertise, and that there is ample room for improving and extending the current description of the biological components. Nevertheless, our intention is not to wander off into this uncharted territory—with reasonable chances of going astray—but to make an inventory of what is currently available, i.e. to provide an overview of how indirect interactions are implicit in the present approach to reactive transport in surface sediments. So, our goal is not to present a new modelling approach, but to investigate the possibilities and limitations of the present diagenetic model formulations as an ecosystem model.

Rather than providing a review, we thought it would be more efficient to present an example model application. Excellent reviews of early diagenetic modelling theory and its applications can be found elsewhere (Berner, 1980; Van Cappellen et al., 1993; Van Cappellen and Gaillard, 1996; Boudreau, 1997, 2000; Giles, 1997; Soetaert et al., 2002). The model presented has the typical structure and formulation of the class of diagenetic models that has emerged over the last 10 years (Soetaert et al., 1996a; Boudreau, 1996a; Van Cappellen and Wang, 1996; Wijsman et al., 2001; Berg et al., 2003; Meysman et al., 2003b). Nevertheless, it adopts a strongly simplified picture of OM diagenesis, as our aim is to illustrate how indirect interactions can be modelled, not to provide a complete representation of OM diagenesis. For this purpose, the inclusion of two competing terminal electron acceptor pathways (oxic respiration and sulphate reduction) suffices. Adding more pathways would not alter the treatment conceptually, but would unnecessarily increase the mathematical burden. As shown below, even for this simplified model the ensuing parameter analysis can become quite intricate.

As model output, we observe a number of biogeochemical variables that would be denoted "ecosystem functions" in the more ecological-oriented literature (e.g. $O_2$ flux across the sediment–water interface (SWI), the partitioning of OM mineralization over oxic and anoxic pathways). The model predicts the steady-state values of these variables for a load of OM that ranges from deep-sea to near-shore conditions. The sensitivity of these "ecosystem functions" is then tested against the occurrence of various "model organisms", through a sensitivity analysis of the biological parameters in the diagenetic model. In order to corroborate the results of numerical simulations, we compare them to simplified theoretical results that are

based on "back-of-the-envelope" first-order approximations. Up to the present, parameter studies of diagenetic models have predominantly focused on geochemical issues, such as the preservation and burial of organic carbon (e.g. Aller and Mackin, 1984; Emerson et al., 1985) and exchange across the SWI (e.g. Cai and Sayles, 1996; Soetaert et al., 1996b). Here, we take the opportunity to perform a systematic exploration of the biological parameter space of a numerical diagenetic model and to evaluate the results in the light of microbial and macrofaunal interactions, i.e. from an ecological perspective.

## Model Description

Our simplified model includes five functional groups, i.e. three microorganisms (oxic respirers, sulphate reducers, sulphide oxidizers) and two macroorganisms (small bioturbators and large bioirrigators). Although this "organism" concept might seem overly simplistic, some real living bacteria and macrofauna species can be linked to the model organisms (Table 1). Microbial activity is represented by the following reactions (Fenchel et al., 1998):

$$R_1 : CH_2O + O_2 \rightarrow HCO_3^- + H^+ \quad (1)$$

$$R_2 : CH_2O + \tfrac{1}{2}SO_4^{2-} \rightarrow HCO_3^- + \tfrac{1}{2}HS^- + \tfrac{1}{2}H^+ \quad (2)$$

TABLE 1. Ecosystem model components: five functional groups and their biogeochemical effects.

| Code | Type | Functional group | Description | Example |
|---|---|---|---|---|
| [1] | Micro | Heterotrophic aerobic respirers | Bacteria that carry out the aerobic mineralization of organic matter ($O_2$ is the terminal electron acceptor) | Pseudomonas |
| [2] | Micro | Heterotrophic sulphate reducers | Bacteria that carry out the anaerobic mineralization of organic matter using sulphate as the terminal electron acceptor | Desulfobacter, Desulfovibrio (typically in a consortium with fermenters) |
| [3] | Micro | Autotrophic sulphide oxidizers | Bacteria that perform the complete aerobic oxidation of sulphide to sulphate | Thiobacillus, Beggiatoa, Thioplaca |
| [4] | Macro | Sediment bioturbators | Small, mobile macroorganisms that thoroughly mix the solid sediment matrix without significantly ventilating the sediment | Notomastus |
| [5] | Macro | Porewater bioirrigators | Large, sedentary organisms that live deep in the sediment, and thus require and induce a high rate of bioirrigation (for simplicity, the occasional solid mixing upon relocation is neglected for these species) | Bivalves (Macoma), sedentary polychaetes (Arenicola) |

$$R_3 : HS^- + 2O_2 \rightarrow SO_4^{2-} + H^+ \tag{3}$$

Reactions $R_1$ and $R_2$ describe the decay of OM (represented as $CH_2O$), fuelling the heterotrophic metabolism of the aerobic respirers and sulphate reducers, respectively. Reaction $R_3$ models the autotrophic metabolism of sulphide-oxidizing bacteria, which re-oxidize the sulphide generated in the process of sulphate reduction.

The activity of macroorganisms is incorporated in the classical way by including a bioturbation and irrigation term in the transport part of the conservation equation. Bioturbation is assumed to affect both porewater and solid-phase "particles". Implementing a random-walk model of particle mixing, the flux due to bioturbation of the *i*th constituent is given by Fick's first law (Guinasso and Schink, 1975; Boudreau, 1986; Meysman et al., 2003a)

$$F_i^{bio} = -\Phi D_b \frac{\partial C_{OM}}{\partial x} \tag{4}$$

where $D_b$ is the biodiffusion coefficient ($cm^2\ yr^{-1}$) and the generic symbol $\Phi$ denotes the appropriate volume fraction (i.e. the porosity $\phi$ for solutes or the solid-phase fraction $1-\phi$ for solid constituents). The $x$-coordinate axis is tied to the SWI and points downwards. Irrigation due to large macrofauna is modelled via a source/sink expression (Emerson et al., 1984; Boudreau, 1984; Koretsky et al., 2002)

$$I_i^{bio} = \alpha \left( C_i^0 - C_i \right) \tag{5}$$

where $\alpha$ denotes the irrigation constant ($yr^{-1}$) and $C_i^0$ denotes the solute concentration at the SWI. We will assume that the bioturbation coefficient $D_b$ and the irrigation coefficient $\alpha$ are constant with time and depth. The independence of time is justifiable, as it implies a stable macrofaunal population with a constant activity. However, the assumption that $D_b$ and $\alpha$ remain constant with depth is a very coarse one. Macrofaunal density typically decreases with depth, and hence macrofaunal activity typically fades at 10–15 cm depth. Yet, this decrease is due to a complex interplay of ecological factors and environmental constraints (depletion of food resources, the increasingly difficult supply of oxygen, the presence of toxic sulphide, and so forth). At present, the actual feedback mechanism from the environment on bioturbation and bioirrigation activity is poorly understood. As a result, diagenetic models do not formulate biological transport as a function of the geochemical environment; i.e. $D_b$ and $\alpha$ are not dependent on concentrations of chemical constituents (except as mentioned earlier: Burdige and Dhakar, 1996; Boudreau, 1998; Herman et al., 1999; Dauwe et al., 2001). Instead, the parameters $D_b$ and $\alpha$ are given a predetermined depth dependence that reflects the decrease of biological activity with depth. Compared to keeping the parameters constant with depth, the latter approach undoubtedly enables a more realistic description of OM diagenesis. However, with regard to our discussion on ecological interactions, it does not bring significant additional value, as it does not allow a feedback of microbiology on macrofauna. At the same time, the degrees of freedom in the model are increased as additional parameters must be included to describe the shape of the $D_b$ and $\alpha$ depth profile. Here, our principal aim is to evaluate the effect of the absence/presence of certain macrofauna (solid bioturbators versus porewater irrigators). As a consequence, we make abstraction of any dependence on depth of the activity of these organisms and concentrate on the response of the model to changes in the overall intensity of bioturbation and bioirrigation.

For our model analysis, we are particularly interested in the steady-state depth profiles of OM, oxygen, sulphate, and sulphide. Assembling the microbial reactions (1)–(3) and

the macrofaunal transport (4)–(5), we obtain the resulting set of steady-state mass conservation equations for these chemical species:

$$D_b \frac{\partial^2 C_{OM}}{\partial x^2} - w\frac{\partial C_{OM}}{\partial x} - R_{min} = 0 \tag{6}$$

$$D^s_{O_2} \frac{\partial^2 C_{O_2}}{\partial x^2} - v\frac{\partial C_{O_2}}{\partial x} + \alpha(C^0_{O_2} - C_{O_2}) - R_1 - 2R_3 = 0 \tag{7}$$

$$D^s_{HS^-} \frac{\partial^2 C_{HS^-}}{\partial x^2} - v\frac{\partial C_{HS^-}}{\partial x} + \alpha(C^0_{HS^-} - C_{HS^-}) + \frac{1}{2}R_2 - R_3 = 0 \tag{8}$$

$$D^s_{SO_4^{2-}} \frac{\partial^2 C_{SO_4^{2-}}}{\partial x^2} - v\frac{\partial C_{SO_4^{2-}}}{\partial x} + \alpha(C^0_{SO_4^{2-}} - C_{SO_4^{2-}}) - \frac{1}{2}R_2 + R_3 = 0 \tag{9}$$

where $v$ and $w$ denote the advective velocities (cm $yr^{-1}$) of the pore water and solid sediment, respectively. In the derivation of (6)–(9), we have adopted the simplifying assumption of constant porosity. The effective diffusion coefficients $D^s$ are calculated from the molecular diffusion coefficients at infinite dilution using the modified Weissberg relation (Boudreau, 1996b)

$$D^S = D^{mol}(T)/(1-2\log\phi) \tag{10}$$

The molecular diffusion coefficients $D^{mol}(T)$ are evaluated at the temperature $T = 6°C$ according to the formulas provided in Boudreau (1997). The resulting values are 265.2, 262.5, and 136.8 $cm^2\ yr^{-1}$ for $O_2$, $HS^-$, and $SO_4^{2-}$ respectively.

The set of diagenetic equations harbours the reaction rates $R_{min}$ and $R_1$–$R_3$, for which we need to provide appropriate kinetic expressions. Following the usual convention, the total mineralization rate is assumed to be first-order in the concentration of degradable OM (Berner, 1964; Westrich and Berner, 1984):

$$R_{min} = kC_{OM} \tag{11}$$

The rates of aerobic respiration and sulphate reduction are then respectively given by (Boudreau, 1992; Van Cappellen and Gaillard, 1996; Soetaert et al., 2002)

$$R_1 = \frac{C_{O_2}}{C_{O_2} + K_{O_2}}\xi R_{min} \tag{12}$$

$$R_2 = \left(1 - \frac{C_{O_2}}{C_{O_2} + K_{O_2}}\right)\xi R_{min} = \frac{K_{O_2}}{C_{O_2} + K_{O_2}}\xi R_{min} \tag{13}$$

Expression (12) incorporates a saturation-type dependence on the oxygen concentration, where $K_{O_2}$ is the saturation constant (Van Cappellen et al., 1993; Boudreau, 1997). This formulation ensures that when oxygen becomes limiting, aerobic mineralization is reduced. When the oxygen concentration is "high", i.e. $C_{O_2} \gg K_{O_2}$, the rate becomes independent of the oxygen concentration. Conversely, when $C_{O_2} \ll K_{O_2}$, the reaction rate $R_1$ becomes linearly dependent on the oxygen concentration. Similarly, expression (13) incorporates an inhibition-type dependence, which suppresses sulphate reduction when oxygen is still available (Van Cappellen et al., 1993; Boudreau, 1997). To keep expression (13) simple, we do not include a saturation-type dependence on the sulphate concentration. Consequently,

we assume that the carbon loading to the sediment stays under the level where sulphate becomes limiting. In other words, all OM that is not going through the oxic pathway (12) is processed by sulphate reduction

$$R_1 + R_2 = \xi R_{min} \tag{14}$$

To ensure the consistency of units between solutes (μM) and solids (μmol $g^{-1}$ of solid sediment), expressions (12)–(14) incorporate the conversion factor $\xi$

$$\xi = \frac{\rho(1-\phi)}{\phi} \times 10^3 \tag{15}$$

where $\rho$ is the solid-phase density (g $cm^{-3}$) and $\phi$ denotes the porosity. The rate of sulphide reoxidation is modelled using the second-order kinetic expression (Millero et al., 1987)

$$R_3 = k_{HS^- - O_2} C_{O_2} C_{HS^-} \tag{16}$$

where $k_{HS^- - O_2}$ is the kinetic rate constant. In order to be able to compare fluxes and reaction rates, we introduce $\hat{R}_{min}$ as the depth-integrated rate of carbon mineralization, $\hat{R}^{OR}_{min}$ and $\hat{R}^{SR}_{min}$ as the respective depth-integrated rates of oxic respiration and sulphate reduction, and $\hat{R}^{SO}_{min}$ as the depth-integrated rate of sulphide oxidation (all in units of μmol $cm^{-2}$ $yr^{-1}$)

$$\hat{R}_{min} = \int_0^L \rho\,(1-\phi)\,R_{min}\,dx \tag{17}$$

$$\hat{R}^{OR}_{min} = \int_0^L 10^{-3}\phi R_1\,dx = \int_0^L \rho(1-\phi)\frac{C_{O_2}}{C_{O_2} + K_{O_2}} R_{min}\,dx \tag{18}$$

$$\hat{R}^{SR}_{min} = \int_0^L 10^{-3}\phi R_2\,dx = \int_0^L \rho(1-\phi)\frac{K_{O_2}}{C_{O_2} + K_{O_2}} R_{min}\,dx \tag{19}$$

$$\hat{R}^{SO} = \int_0^L 10^{-3}\phi R_3\,dx \tag{20}$$

The link between the total mineralization of OM and the total rates of the different pathways is given by the relation

$$\hat{R}^{min} = \hat{R}^{OR} + \hat{R}^{SR} \tag{21}$$

which also directly follows from the integration of expression (14).

## Boundary Conditions

The flux of organic carbon $F^0_{OM}$ (expressed in mmol C $cm^{-2}$ $yr^{-1}$) arriving at the SWI is assumed constant, leading to following Robin-type boundary condition:

$$F^0_{OM} = \rho(1-\phi)\left[-D_b \frac{\partial C_{OM}}{\partial x} + w C_{OM}(x)\right]_{x=0} \tag{22}$$

The concentrations of the solute species are prescribed at the SWI, leading to the Dirichlet-type boundary condition

$$C_i\big|_{x=0} = C_i^0 \tag{23}$$

where $i = HS^-$, $SO_4^{2-}$, $O_2$. At the lower boundary $x = L$, it is assumed that all gradients vanish, so solutes and solids are transported by advection only. Consequently, the following Neumann-type boundary condition is imposed:

$$\left.\frac{\partial C}{\partial x}\right|_{x=L} = 0 \tag{24}$$

for all four model constituents.

## Model Solution

A simulation involves the calculation of the concentration profiles of $CH_2O$, $O_2$, $SO_4^{2-}$ and $HS^-$ according to the differential equations (6)–(9) for a given set of parameters. Table 2 provides an overview of the parameter values that were implemented in the various ecosystem models presented below. In all simulations presented here, the model domain extends to a depth of L = 30 cm. The mass balance (6) for OM is not coupled to the other three equations (7)–(9), and hence it proves the only equation for which an analytical solution is possible.

TABLE 2. Overview of the parameter set of the ecosystem model. Parameter values in bold type denote values that belong to the standard simulation setting.

| | | | |
|---|---|---|---|
| **Geometrical parameters** | | | |
| Depth of modelled sediment layer | L | 30 | cm |
| Depth of bioturbated layer | $L_B$ | 30 | cm |
| Depth of bioirrigated layer | $L_I$ | 30 | cm |
| **Environmental parameters** | | | |
| Temperature | T | 6.0 | °C |
| Porosity | $\phi$ | 0.8 | - |
| Solid-phase density | $\rho$ | 2.55 | g $cm^{-3}$ |
| **Transport parameters** | | | |
| Advective velocity (solutes) | V | 0.1 | cm $yr^{-1}$ |
| Advective velocity (solids) | $\omega$ | 0.1 | cm $yr^{-1}$ |
| Bioturbation coefficient | $D_b$ | 0, 0.1, **1.0**, 10 | $cm^2$ $yr^{-1}$ |
| Bioirrigation intensity | $\alpha$ | **0**, 1.58, 15.8, 158, 1580 | $yr^{-1}$ |
| **Reaction parameters** | | | |
| OM decay constant | k | 0.01, 0.03, **0.1**, 0.3, 1.0 | $yr^{-1}$ |
| Monod constant $O_2$ | $K_{O_2}$ | 0.31, **3.1**, 31, 310 | µM |
| Sulphide oxidation constant | $K_{HS^-O_2}$ | 0, 0.22, 2.2, 22, **220** | $\mu M^{-1}$ $yr^{-1}$ |
| **Boundary parameters** | | | |
| Flux OM at SWI | $F_{OM}^0$ | 0–0.6 | mmol C $cm^{-2}$ $yr^{-1}$ |
| Concentration at SWI | $C_{O_2}^0$ | 295 | µM |
| Concentration at SWI | $C_{SO_4^{2-}}^0$ | 28,000 | µM |
| Concentration at SWI | $C_{HS^-}^0$ | 0 | µM |

The steady-state solution to the advection–diffusion equation (6) with kinetic expression (11) and boundary conditions (22) and (24) is given by (Crank, 1975; Boudreau, 1997)

$$C_{OM}(x) = C^0_{OM} \exp\left(-\frac{x}{\bar{x}}\right) \tag{25}$$

where $C^0_{OM}$ is the concentration at the SWI, and $\bar{x}$ is a characteristic depth, defined respectively as

$$C^0_{OM} = \frac{2F^0_{OM}}{\rho(1-\phi)\left[w + \sqrt{w^2 + 4D_b k}\right]} \tag{26}$$

$$\bar{x} = \frac{2D_b}{-w + \sqrt{w^2 + 4D_b k}} \tag{27}$$

To keep the expression (25) simple, we have assumed a semi-infinite domain, i.e. $L = +\infty$ in expression (24). When burial of OM is negligible, i.e. when all the OM decays within the model domain, one obtains that

$$\hat{R}_{min} \approx F^0_{OM} \tag{28}$$

which formally states that the depth-integrated mineralization equals the flux of labile OM. To check this condition, we can introduce the penetration depth of OM, $\delta_{OM}$, as the depth where the OM concentration decreases to 1% of its value at the SWI. Employing (25), we immediately find that $\delta_{OM}$ is about 5 times the characteristic depth

$$\delta_{OM} = -\bar{x} \ln\left[\frac{C_{OM}(\delta_{OM})}{C^0_{OM}}\right] = -\bar{x} \ln[0.01] \approx 5\bar{x} \tag{29}$$

Equation (29) can be used to calculate the minimal decay constant necessary to ensure full OM degradation within the model domain L. For a model domain of L = 30 cm and the standard values $w = 0.1$ cm yr$^{-1}$ and $D_b = 1$ cm$^2$ yr$^{-1}$ employed in the simulations, we arrive at a minimal decay constant $k_{min} = 0.044$ yr$^{-1}$. To ensure full OM mineralization, we adopted $k = 0.1$ yr$^{-1}$ as the default value in the simulations (see below).

The presence of the OM concentration in the kinetic rate expressions (12) and (13) couples the conservation equations for $O_2$ and $SO_4^{2-}$ to that of OM via expression (11). In addition, expressions (12) and (13) are non-linear due to the saturation term. The kinetic rate expression for sulphide oxidation (16) couples the equations for $O_2$ and $HS^-$ in a similar way. Both the coupling and non-linearity generally prevent an analytical solution to the mass balances (7)–(9). Consequently, we employed the Chemical Engineering (CE) Module within the finite element package FEMLAB (COMSOL, 2002) to pursue a numerical solution. The CE Module has a pre-programmed equation mode called "convection and diffusion" which makes it very suitable for solving the system of non-linear differential equations (7)–(9). Note that the bioirrigation term (4) has the form of a "source/sink", and therefore, should be treated formally as a reaction term. A non-uniform finite element (quadratic elements) grid was used. In the vicinity of SWI where large concentration gradients are expected, an element size of 0.1 mm is used, while the grid resolution is decreased

10 times towards the lower boundary. The FEMLAB solver setting was put to "highly nonlinear", which resulted in very moderate CPU requirements for our one-dimensional simulations (on the order of seconds to 1 min, depending on parameters and boundary conditions). For the integration and interpolation of variables over the computational domain, the built-in postprocessing functions of FEMLAB were used.

## Results

Rather than analyzing the full ecosystem model (1)–(24) at once, we will proceed in a sequential fashion by adding one "model organism" at a time. In the most basic simulation, only the two heterotrophic bacteria are incorporated. This will allow us to investigate the competitive partitioning of OM processing between these two "microorganisms". Once this basic setting is fully analyzed, we extend the ecosystem model by the sequential addition of new functional groups. First, the autotrophic sulphide oxidizers are incorporated, and the influence of their presence on the heterotrophic bacteria is investigated. Subsequently, the two macrofaunal species are included, which enables us to investigate the influence of macrofaunal transport on microbial ecology.

Note that we do not imply that all the model ecosystems in this sequence bear relevance for actual sediments (whether laboratory set-ups or in situ sediments). In particular, the basic setting of only two heterotrophic bacteria with no other bacteria that reoxidize reduced mineralization products is barely credible. Nevertheless, we see the creation of such virtual ecosystems exactly as the advantage of the present modelling exercise. We can gradually build up the complexity and investigate the effects of adding new model organisms one-by-one.

### *(1) Interactions Between Different Heterotrophic Bacteria*

The incorporation of the two mineralization pathways $R_1$ and $R_2$ in our ecosystem model simulates the competition between two heterotrophic bacterial communities for OM substrate. Classically, the outcome of such competition between bacterial communities is linked to the standard free energy of the associated metabolic processes. Based on the aerobic degradation of glucose, one can calculate a standard free energy $\Delta G^0 = -479$ kJ mol$^{-1}$ for reaction $R_1$, and $\Delta G^0 = -265$ kJ mol$^{-1}$ for reaction $R_2$ (Fenchel et al., 1998). Clearly, aerobic oxidation of OM is favoured over sulphate reduction from a thermodynamic point of view. This competitive exclusion is modelled by the interplay of the saturation term $C_{O_2}/(C_{O_2} + K_{O_2})$ for aerobic mineralization in (12) and the inhibition term $K_{O_2}/(C_{O_2} + K_{O_2})$ for sulphate reduction in (13) (Van Cappellen et al., 1993). As noted previously, the latter is simply one minus the former. This way, the overlap between the zones of aerobic mineralization and sulphate reduction is determined by a single parameter, i.e. the saturation constant $K_{O_2}$. A small value of $K_{O_2}$ results in a sharp transition of the associated bacterial activities, whereas a large $K_{O_2}$ creates a wide overlap.

Of particular interest is the proportion of OM that is processed by either aerobic or anaerobic mineralization in relation to the flux of organic carbon arriving at the SWI. In other words, how do the aerobic-respiring community (whose extent is characterized by $\hat{R}^{OR}_{min}$) and the sulphate-reducing community (characterized by $\hat{R}^{SR}_{min}$) change as a function of $F^0_{OM}$? In Figure 1 we depict the output of a sweep simulation, in which $F^0_{OM}$ ranges from deep-sea ($F^0_{OM}$ = 0.01 mmol C cm$^{-2}$ yr$^{-1}$) to coastal conditions ($F^0_{OM}$ = 0.6 mmol C cm$^{-2}$ yr$^{-1}$). The horizontal axis in Figure 1 can also be regarded as the inverse of the water column depth or

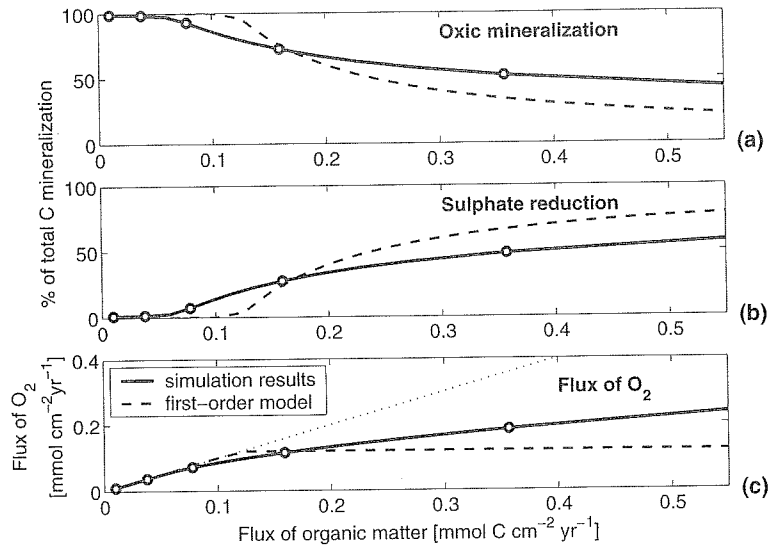


Figure 1. Two-species ecosystem (aerobic respirers + sulphate reducers). Dependence of the mineralization pathways and the oxygen flux on the flux of organic matter (OM) in the absence of sulphide oxidation ($k_{HS^- - O_2} \equiv 0$), bioturbation ($D_b \equiv 0$), and bioirrigation ($\alpha \equiv 0$). The solid lines denote the numerical solution to the equations (6)–(9). The dashed lines represent the output from the approximate model as explained in the text. The straight, light dotted line in panel c represents the one-to-one ratio between fluxes of OM and oxygen. Fixed parameter values: $k = 0.1$ yr$^{-1}$, $K_{O_2} = 3.1$ μM. Circles refer to specific simulations depicted in Figure 2.

the distance from the shoreline. In the simulations of Figure 1, we used fixed values for the saturation constant $K_{O_2} = 3.1$ μM, the decay constant of OM $k = 0.1$ yr$^{-1}$, and the advective velocities $v = w = 0.1$ cm yr$^{-1}$. The porosity is given the constant value $\phi = 0.8$, reflecting an average value for the top 20 cm of muddy environments. As we consider the effect of only heterotrophic bacteria in this first ecosystem model, we have shut down the activity of sulphide-oxidizing bacteria (i.e. $k_{HS^- - O_2} \equiv 0$), as well as bioturbation (i.e. $D_b \equiv 0$) and bioirrigation (i.e. $\alpha \equiv 0$) by macrofauna. Due to the absence of reoxidation and bioirrigation, the diffusive oxygen flux at the SWI essentially matches the total oxic mineralization, i.e. $F^0_{O_2} \approx \hat{R}^{OR}_{min}$. Similarly, the integrated rate of sulphate reduction must equal half the flux of sulphide lost to the water column through the SWI, i.e. $F^0_{HS^-} \approx 2\hat{R}^{SR}_{min}$. The equality sign in both expressions is not strict, because a small loss occurs due to the downward advection of porewater, leading to a small flux of oxygen and sulphide to the underlying sediment.

Figure 1 depicts the responses of the following ecosystem functions to increased carbon loadings: (1) the partitioning between oxic and anoxic pathways, and (2) the oxygen flux to the sediment across the SWI. To interpret the results from our numerical simulations, it is useful to compare them to following simplified two-regime scenario of OM processing (referred to as the first-order model in Figure 1). In a first regime, for small carbon loadings, we assume the sediment is completely oxic, and hence, all mineralization occurs through the oxic pathway

$$\hat{R}^{OR}_{min} = F^0_{OM} \quad \text{and} \quad \hat{R}^{SR}_{min} = 0 \tag{30}$$

The oxygen flux adapts to the amount of oxygen required in the oxic mineralization process, i.e. $F^0_{O_2} \approx \hat{R}^{OR}_{min}$ (dashed line in Figure 1c up to 0.13 mmol C $cm^{-2}$ $yr^{-1}$). This situation remains unaltered until the flux of organic carbon passes a certain threshold. Beyond this "switching point", diffusional transport from the overlying water column is no longer capable of supplying sufficient oxygen to compensate for the electron acceptor demand from OM decay. In this second regime, oxygen is exhausted at depth in the sediment and sulphate reduction switches on to "fill the electron acceptor gap". In our (oversimplified) first-order model, we further assume that the oxygen flux remains invariant beyond the "switching point". Accordingly, the total aerobic respiration will remain constant for increasing fluxes of OM (dashed line in Figure 1c beyond 0.13 mmol C $cm^{-2}$ $yr^{-1}$), and the total rate of sulphate reduction will linearly scale with the flux of organic carbon, albeit diminished by the constant factor, i.e.

$$\hat{R}^{OR}_{min} = F^0_{O_2} \quad \text{and} \quad \hat{R}^{SR}_{min} = F^0_{OM} - F^0_{O_2} \tag{31}$$

Expressed relatively, the share of oxic respiration in the total mineralization will inversely decrease (dashed line Figure 1a), while the share of sulphate reduction will increase (dashed line in Figure 1b).

Remarkably, the numerical simulation results (Figure 1, solid line) diverge appreciably from those predicted by the simplified two-regime model (Figure 1, dashed line) in two ways. The onset of sulphate reduction occurs at lower organic carbon loadings than expected, while at high organic carbon loadings, the rate of oxic mineralization is higher than expected. These deviations provide a first clear example of how the coupling of conservation equations complicates the interpretation of the model output. The earlier onset of sulphate reduction is relatively easy to understand and can be attributed to the presence of the saturation terms in the kinetic expressions (11) and (12) for the metabolic pathways. Due to this saturation formulation, the oxygen at depth does not have to vanish completely in order to allow sulphate reduction.

In contrast, the increased oxic mineralization rate at higher organic loadings requires a more detailed explanation. Upon substitution of the kinetic expressions (11) and (12) into the equation for the total oxic respiration rate (18), one can make the following approximation

$$F^0_{O_2} \approx \hat{R}^{OR}_{min} = \int_0^{\delta_{O_2}} \rho(1-\phi)\frac{C_{O_2}}{C_{O_2} + K_{O_2}} k C_{OM} dx \approx \rho(1-\phi) k \bar{C}_{OM} \delta_{O_2} \tag{32}$$

where $\bar{C}_{OM}$ denotes the average concentration of OM *in the oxic zone* of the sediment and $\delta_{O_2}$ the oxygen penetration depth. Because the saturation constant $K_{O_2}$ is low, $C_{O_2} > K_{O_2}$ holds over most of the oxic zone, and hence we can remove the monod term from the integral in (32). To analyze expression (32), one needs an estimate for both the quantities $\bar{C}_{OM}$ and $\delta_{O_2}$. To calculate $\bar{C}_{OM}$, we can use the solution of an advection–decay model (i.e. the analytical solution (25) with $D_b \equiv 0$), to obtain

$$\bar{C}_{OM} \equiv \frac{1}{\delta_{O_2}} \int_0^{\delta_{O_2}} C_{OM}(x) dx = C^0_{OM} \frac{\bar{x}}{\delta_{O_2}} \left[ 1 - \exp\left( -\frac{\delta_{O_2}}{\bar{x}} \right) \right] \tag{33}$$

At high carbon loadings, the oxygen penetration depth becomes small (Figure 2b), and under this condition, the exponential term in (33) can be linearly approximated as

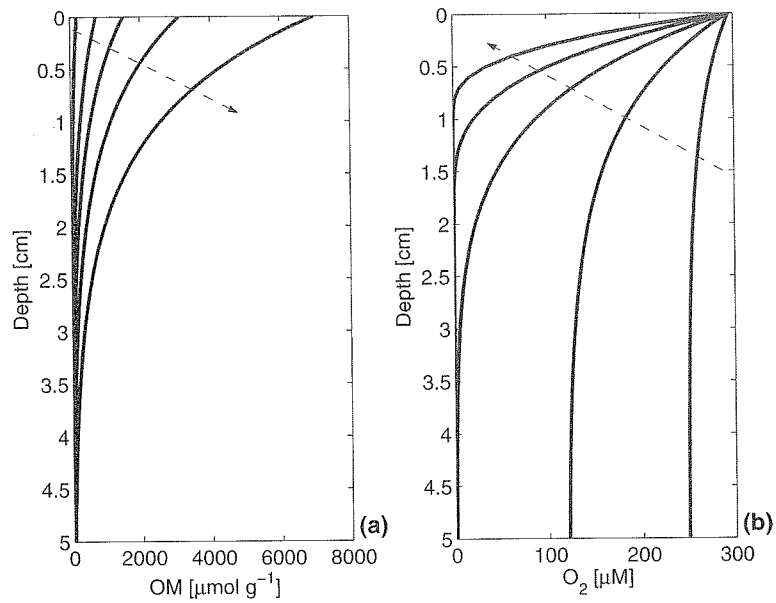


Figure 2. Depth profiles (upper 5 cm) for the concentration of OM (left panel) and oxygen (right panel), obtained for the OM fluxes indicated by the circular markers in Figure 1. The arrows represent the trend with an increase of the OM flux.

$\exp(-\delta_{O_2}/\bar{x}) \approx 1-\delta_{O_2}/\bar{x}$. Substituting this result in (33), we find that $\bar{C}_{OM} \approx C^0_{OM}$; i.e. the concentration of OM does not vary much over the oxic zone and equals that at the interface. Substituting (33) into (32), and noting that according to (26) $C^0_{OM} = F^0_{OM}/\left[\rho(1-\phi)w\right]$, one arrives at

$$F^0_{O_2} \approx \frac{k}{w}\delta_{O_2}F^0_{OM} \tag{34}$$

Formula (34) indicates that the oxygen flux will increase with increased carbon loading. However, the only way the flux of oxygen $F^0_{O_2}$ can increase is with a decrease of the oxygen penetration depth $\delta_{O_2}$. Basically, the fixed concentration $C^0_{O_2}$ at the SWI acts as a pivot for the oxygen flux $F^0_{O_2}$. Consequently, there is a manifestation of two opposite tendencies in expression (34); i.e. when $F^0_{OM}$ increases, $\delta_{O_2}$ decreases. These conflicting tendencies essentially originate from the coupling of the mass conservation equations of oxygen (7) and organic carbon (6) through kinetic expressions (11)–(12). Expression (34) provides a clear example of how non-linear effects are often introduced by coupling, and how these complicate the interpretation of results.

The dominant trend in the oxygen flux can be extracted from following alternative expression for the oxygen flux:

$$F^0_{O_2} = -\phi D^s_{O_2}\left.\frac{\partial C}{\partial x}\right|_{x=0} \approx -\phi D^s_{O_2}\frac{C_{O_2}(\delta)-C^0_{O_2}}{\delta_{O_2}} = \phi D^s_{O_2}\frac{C^0_{O_2}}{\delta_{O_2}} \tag{35}$$

The depth $\delta_{O_2}$ now represents the intercept of the derivative of the oxygen concentration with the $x$-coordinate axis and hence must be interpreted as a *scale indicator* for the penetration depth of oxygen (Di Toro et al., 1990; Cai and Sayles, 1996). Based on a more elaborate second-order polynomial model for the oxygen concentration, one can show that the actual oxygen penetration depth, i.e. the location where the oxygen concentration vanishes, is a factor of two larger (Bouldin, 1968; Cai and Sayles, 1996; Di Toro, 2001). The implementation of this second-order model would increase the complexity of our presentation but would not affect the parameter analysis and the resulting conclusions. Consequently, we will retain the first-order approximation (35) and hereafter refer to $\delta_{O_2}$ as the oxygen penetration depth. Equating the expressions (34) and (35) leads to the following estimate for the oxygen penetration depth:

$$\delta_{O_2} \approx \sqrt{\phi D_{O_2}^S \frac{w C_{O_2}^0}{k F_{OM}^0}} \tag{36}$$

Substituting (36) into (34), one obtains following final expression for the oxygen flux:

$$\hat{R}_{min}^{OR} \approx F_{O_2}^0 \approx \sqrt{\phi D_{O_2}^S C_{O_2}^0 \frac{k}{w} F_{OM}^0} \tag{37}$$

Note that expression (37) has identical dependencies as the formula obtained by Bouldin (1968), Cai and Sayles (1996) and Di Toro (2001) based on the second-order model, but for a scaling factor $\sqrt{2}$. Expression (37) resolves the conflicting tendencies between $F_{OM}^0$ and $\delta_{O_2}$ in (34). The overall tendency is an increase in the total oxygen flux $F_{O_2}^0$—or equally the oxic mineralization rate $\hat{R}_{min}^{OR}$—with increasing carbon loading (Figure 1c). Also, the original tenet of our "back-of-the-envelope" two-regime model, i.e. that $F_{O_2}^0$ remains constant past the switching point, is now deemed unjustified (solid line as opposed to dashed line in Figure 1c). Assuming total OM degradation (28), $\hat{R}_{min}^{SR}$ can be calculated from (37) as

$$\hat{R}_{min}^{SR} \approx F_{OM}^0 - \hat{R}_{min}^{OR} = F_{OM}^0 - \sqrt{\phi D_{O_2}^S C_{O_2}^0 \frac{k}{w} F_{OM}^0} \tag{38}$$

The fraction $\beta$ of the total mineralization that is due to aerobic mineralization becomes

$$\beta = \frac{\hat{R}_{min}^{OR}}{\hat{R}_{min}^{OR} + \hat{R}_{min}^{SR}} = \frac{\sqrt{\phi D_{O_2}^S C_{O_2}^0 k}}{\sqrt{w F_{OM}^0}} \tag{39}$$

which scales with the inverse square root of the organic carbon flux (Figure 1b).

The previous analysis explains the general dependence of the metabolic pathways partitioning and oxygen flux on the supply of OM to the sediment. In a next step, we can analyse how these profiles change with the quality of OM and the physiology of the bacteria, respectively. The quality of organic carbon is expressed by its decay constant k, and Figure 3 shows how the metabolic partitioning changes with k. For a given flux of OM, the more degradable the OM (i.e. increasing values of k), the more the oxic respiration pathway dominates. Conversely, refractory OM favours sulphate reduction. The explanation of this trend is already contained in expression (37). For a given flux, the total oxygen respiration rate $\hat{R}_{min}^{OR}$ shows a monotonic (square-root) increase with the decay constant k.

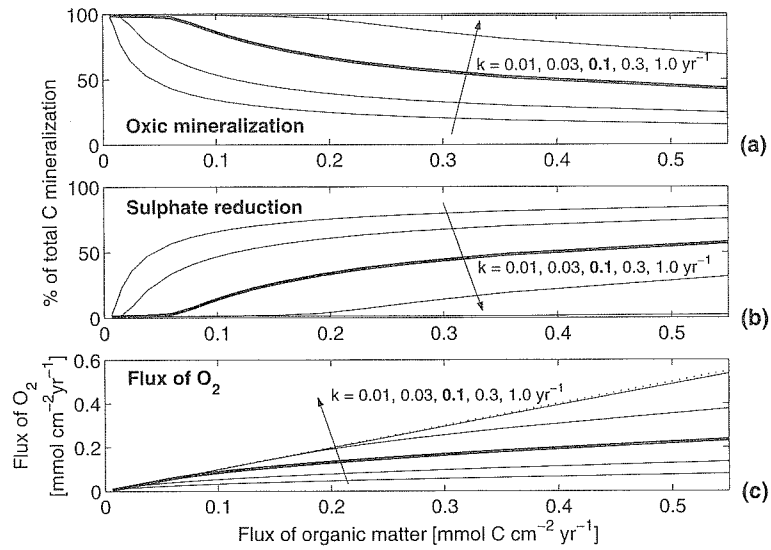


Figure 3. Sensitivity analysis of the model solution of Figure 1 (no sulphide oxidation, no bioturbation, and no bioirrigation) for different values of the mineralization constant k. The bold line in each panel corresponds to the value k = 0.1 yr$^{-1}$, which is used in all subsequent simulations.

Just as we did for k, we can investigate the dependence of the metabolic pathways on the magnitude of the saturation constant. In other words, we can investigate what the effect would be of a physiological change of heterotrophic oxidizers, altering their affinity for oxygen. Figure 4 shows a sensitivity analysis for the $K_{O_2}$. As already noted, the magnitude of the saturation constant $K_{O_2}$ determines the degree of coexistence between the oxic respirers and sulphate reducers. An increased value of $K_{O_2}$ allows the occurrence of sulphate reduction at the expense of aerobic mineralization.

The sensitivity analysis for k has one more aspect worth discussing. Figure 3 shows that for a sufficiently high k value, the mineralization of OM thus becomes completely oxic, even for highly carbon loaded sediments. The reason for this is that the mineralization is so rapid that all OM degradation is concentrated in a narrow zone near the SWI, which is smaller than the oxygen penetration depth. As seen from Figure 3, this situation occurs when k values exceed 1 yr$^{-1}$, which is high, but not unreasonably high. In other words, if all the organic carbon arriving at a muddy coastal site were in the form of glucose, our model would predicts this site to be oxic, instead of being anoxic as typically observed in real coastal muds. The question is whether this conclusion bears any realism for coastal environments. Coastal sands (i.e. environments with lower porosities) *are* known to be oxic environments. Yet, their oxic character appears to result from a combination a high reactivity of OM (Dauwe et al., 2001) and, more importantly, a strong advective exchange (Huettel et al., 1998), pumping oxygen into the sediment from the overlying water column (a phenomenon that is beyond the discussion here). Yet, the potential oxic character of coastal muds at k > 1 seems unrealistic. One should recall that this conclusion results from our most basic ecosystem model, with its extensive assumptions. Neither sulphide oxidation nor bioturbation is taken into account, which, as shown below, significantly raises the required k value necessary for complete oxic conditions. Moreover, in natural sediments, OM quality is a distributed parameter with the consequence that high- and low-quality material come

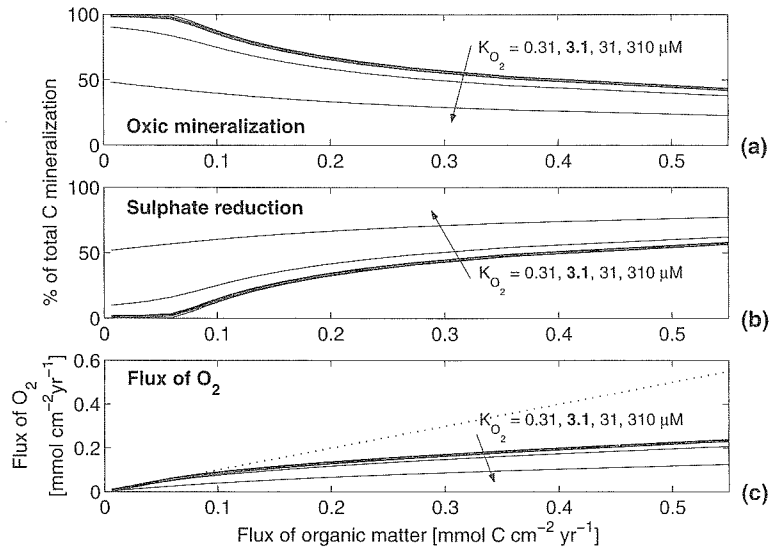


Figure 4. Sensitivity analysis of the model solution of Figure 1 (no sulphide oxidation, no bioturbation, and no bioirrigation) for the different values of the saturation constant $K_{O_2}$. The bold line in each panel corresponds to the value $K_{O_2}$ = 3.1 µM, which is used in all subsequent simulations.

together. So, the apparent k value must be lowered when considering only one bulk fraction. Overall, this paragraph shows a nice example of how oversimplification of models may lead to wrong interpretations. Accordingly, one should never lose sight of the initial model assumptions when interpreting the final model output.

## *(2) Interactions Between Heterotrophic/Autotrophic Bacteria*

To alleviate the criticism of oversimplification, we can extend the basic two-organism ecosystem model of the previous section to incorporate sulphide oxidizers as a third functional group. The geochemical activity of the latter bacteria is characterized by the kinetic constant $k_{HS^- - O_2}$ in reaction $R_3$. Literature values for this kinetic constant diverge radically between the water column and the sediment environment. In the sediment, few values have been reported, but these are systematically several orders of magnitude higher than in the overlying water (Boudreau, 1991). Two explanations can be invoked for this remarkable discrepancy: (1) Sulphide oxidation in the water column is mostly chemical, whereas in the sediment it is thought to be mainly microbial, which proceeds distinctly faster (Buisman et al., 1990). (2) The concentration of bacteria in the sediment (~$10^9$ ml$^{-1}$) is typically three orders of magnitude higher than in the water column (~$10^6$ ml$^{-1}$) (Heip et al., 1995).

Simulations for different values of $k_{HS^- - O_2}$ are presented in Figure 5. First, let us analyse the $O_2$ and $HS^-$ balances for the default simulation where $k_{HS^- - O_2}$ is set to zero (i.e. the model of the previous section). The oxygen flux across the SWI (solid lines in Figures 1c and 5c) lies well below the one-to-one relation with the flux of OM (dotted lines in

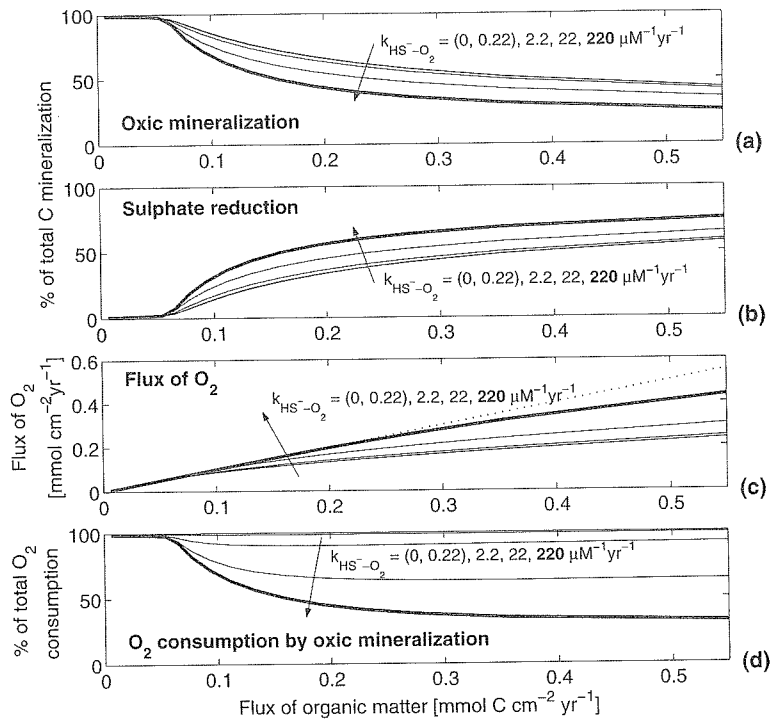


Figure 5. Three-species ecosystem (aerobic respirers + sulphate reducers + sulphide oxidizers). Dependence of the mineralization pathways, the oxygen flux and the percentage of the oxygen consumption by oxic mineralization as a function of the flux of OM. No macrofaunal transport is included: $D_b \equiv 0$ and $\alpha \equiv 0$. The arrows represent the trend with an increase of the kinetic constant for sulphide oxidation. Fixed parameter values: $k = 0.1\ yr^{-1}$, $K_{O_2} = 3.1\mu M$. The parentheses aggregate parameters for which the curves fall together.

Figures 1c and 5c). This discrepancy results from $HS^-$ diffusing out of the sediment across the SWI. Ignoring the small correction due the advective burial of sulphide, this $HS^-$ flux should match the total sulphate reduction rate stoichiometrically, i.e. $\hat{R}^{SR}_{min} \approx 2F^0_{HS^-}$. However, when $k_{HS^-O_2}$ differs from zero, the simple relations $\hat{R}^{OR}_{min} \approx F^0_{O_2}$ and $R^{SR}_{min} \approx 2F^0_{HS^-}$ are no longer valid and should be corrected for the effect of sulphide oxidation.

$$\hat{R}^{OR}_{min} \approx F^0_{O_2} - 2\hat{R}^{SO} \tag{40}$$

$$\hat{R}^{SR}_{min} \approx 2F^0_{O_2} + 2\hat{R}^{SO} \tag{41}$$

Expressions (40) and (41) follow directly from the postulated reaction scheme (1)–(3). Expression (40) denotes that the flux of oxygen penetrating the SWI is consumed due to both oxic respiration and sulphide oxidation. Expression (41) shows that the sulphide produced in sulphate reduction goes either to sulphide reoxidation or is lost across the SWI. The direct implications of expressions (40) and (41) are shown in panels a and b of Figure 5.

Oxic mineralization decreases and sulphate reduction increases with increasing values of $k_{HS^- - O_2}$. At a sufficiently high value of $k_{HS^- - O_2}$, all the sulphide produced by sulphate reduction will be reoxidized to sulphate, and the $HS^-$ flux across the SWI will vanish. In this situation, expression (41) becomes

$$\hat{R}^{SR}_{min} \approx 2\hat{R}^{SO} \tag{42}$$

Substituting (42) into (40), one finds

$$F^0_{O_2} \approx \hat{R}^{OR}_{min} + \hat{R}^{SR}_{min} \tag{43}$$

Consequently, at high enough values of $k_{HS^- - O_2}$, the oxygen flux will match the incoming flux of organic carbon, i.e. the one-to-one lines in Figures 1c and 5c. Figure 5c shows that $k_{HS^- - O_2}$ must be higher than $10^3$ $\mu M^{-1}$ $yr^{-1}$ to achieve this situation of full sulphide oxidation. Higher values of $k_{HS^- - O_2}$ were however not explored, because these engendered numerical instabilities. All the sulphide oxidation is then located in a really narrow reaction zone, beyond the resolution of the finite element grid. Adaptive grid refinement techniques could provide a resolution to this problem.

For the case of full sulphide reoxidation ($k_{HS^- - O_2} = 220$ $\mu M^{-1}$ $yr^{-1}$ in Figure 5), we can evaluate the partitioning between oxic and anoxic pathways, and the oxygen flux to the sediment as a function of the carbon loadings, using a similar first-order procedure as in the previous section. When OM is fully degraded, i.e. expression (28) holds, and all sulphide produced during sulphate reduction is reoxidized, i.e. expression (43) holds, the flux of organic carbon must match that of oxygen, i.e. $F^0_{OM} \approx F^0_{O_2}$. Employing once more the first-order model (35), the oxygen penetration depth can be estimated as

$$\delta_{O_2} \approx \phi D^s_{O_2} \frac{C^0_{O_2}}{F^0_{OM}} \tag{44}$$

Compared to the case of no sulphide reoxidation (36), there are marked differences in the relation for $\delta_{O_2}$. (1) The oxygen penetration depth $\delta_{O_2}$ is dependent only on the oxygen para meters $D^S_{O_2}$ and $C^0_{O_2}$ and the total flux of organic carbon $F^0_{OM}$ and is no longer dependent on the advective velocity $w$ or the quality of the OM k. Accordingly, the actual way how OM is transported and transformed within the sediment no longer influences the oxygen penetration depth. (2) The penetration depth now scales with the inverse of the organic flux $F^0_{OM}$ rather than with the inverse root in (36).

Combining expressions (32)–(34), one arrives at the counterpart expressions for (37) and (38). The total aerobic mineralization and total sulphate reduction now become, respectively

$$\hat{R}^{OR}_{min} \approx \delta_{O_2} \rho (1-\phi) k \bar{C}_{OM} = \phi D^s_{O_2} C^0_{O_2} \frac{k}{w} \tag{45}$$

$$\hat{R}^{SR}_{min} \approx F^0_{OM} - \phi D^s_{O_2} C^0_{O_2} \frac{k}{w} \tag{46}$$

Expression (45) shows no longer a dependence of $\hat{R}^{OR}_{min}$ on the flux of OM. The fraction $\beta$ of the total mineralization that is due to aerobic mineralization is calculated as

$$\beta = \frac{\hat{R}^{OR}_{min}}{\hat{R}^{OR}_{min} + \hat{R}^{SR}_{min}} = \frac{\phi D^s_{O_2} C^0_{O_2} k}{w F^0_{OM}} \tag{47}$$

So, theoretically, we obtain an inverse dependency on the organic carbon flux in the relations (47) for the case of full sulphide reoxidation as opposed to the inverse square root dependency (39) for the case of no sulphide reoxidation. This approximate derivation is corroborated by the numerical simulations in Figure 5a, which show a stronger curvature of the profiles in the case of full sulphide reoxidation. Also Figure 5d shows that for high carbon loadings and full sulphide oxidation, about 30–40% of the oxygen flux is used for aerobic respiration, whereas the bulk part, i.e. 60–70%, is consumed in sulphide reoxidation, consistent with results based on more advanced models (Soetaert et al., 1996a,b) and field observations (Jorgensen, 1982).

Again we should draw attention to an important assumption underlying the present model. Our models results imply that the flux of oxygen into the sediment can always match the oxygen demand from sulphide oxidation. This is because the model imposes a fixed oxygen concentration at the SWI via the boundary condition (23). Accordingly, this concentration acts as a pivot for the oxygen flux; i.e. any demand for oxygen can be counteracted by reducing the oxygen penetration depth and thus increasing the oxygen concentration gradient at the SWI. In other words, OM mineralization within the sediment has no feedback on the oxygen concentration in the overlying water column, and so, the water column effectively can act as an infinite source of oxygen. In reality, sufficiently high mineralization rates and associated sulphide production will have an impact on overlying water chemistry and will lead to oxygen depletion in the near-bottom boundary layer.

### *(3) Interactions Between Microorganisms/Macroorganisms: Bioturbation*

In the previous sections, the effect of three functional groups of bacteria was investigated by including them as chemical reactions in a simple reactive-transport model, where advection and molecular diffusion were the only transport processes considered. We now proceed by evaluating the influence of macrofauna on our ecosystem, particularly on the three functional groups of microorganisms already included. The representation of the macrofauna occurs by including bioturbation and bioirrigation as additional transport processes. Bioturbation is modelled as a "local" transport process via the biodiffusive analogy (4) (Boudreau, 1986; Meysman et al., 2003a), while bioirrigation is incorporated via the non-local formulation (5) (Boudreau, 1984).

In our model, bioturbation is linked to small burrowing worms, which mix both the solid sediment and the porewater due to small-scale, random displacements (Boudreau, 1986; Meysman et al., 2003a). In principle, the biodiffusion coefficient $D_b$ should feature in both the equation for OM (6) and those for the solutes (7)–(9), and the values of the $D_b$ in both phases should not be the same. The diffusive mixing of solids is usually termed biodiffusion, while the additional mixing transport of the porewater is usually termed enhanced porewater diffusion. Here, we will assume the influence of the small bioturbators on the porewater to be small compared with the large bioirrigators analysed in the next section. So, we will not incorporate enhanced diffusion into the model.

Figure 6 shows numerical simulations for different values of $D_b$, all other parameters being fixed. Several aspects are notable with increasing $D_b$: (1) the share of sulphate reduction in total mineralization increases, (2) the OM flux at which sulphate reduction first occurs becomes smaller, (3) the flux of oxygen remains invariant with bioturbation intensity, and (4) the share of aerobic mineralization in the total oxygen consumption decreases at the expense of sulphide reoxidation. To provide a theoretical support for these numerical results, we can follow a similar procedure as in the previous sections. In analogy to the derivation of expression (34), we can first approximate the average concentration of

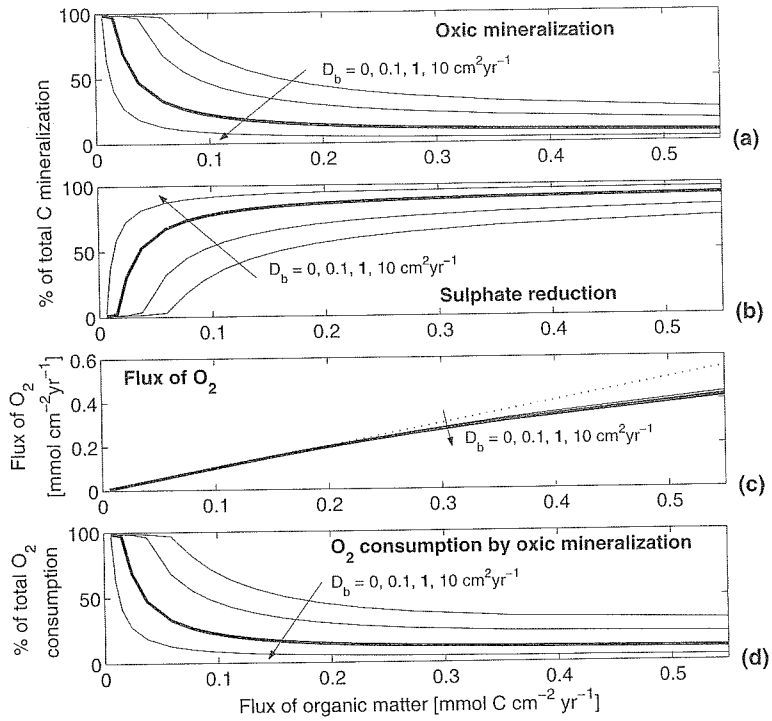


Figure 6. Four-species ecosystem (aerobic respirers + sulphate reducers + sulphide oxidizers + bioturbators). Dependence of the mineralization pathways, the oxygen flux, and the percentage of the oxygen consumption by oxic mineralization as a function of the flux of OM. Bioturbation is the only macrofaunal transport included, i.e. $\alpha \equiv 0$. The arrows represent the trend with an increase of $D_b$. Fixed parameter values: $k = 0.1\ yr^{-1}$, $K_{O_2} = 3.1\ \mu M$, $k_{HS^- - O_2} \equiv 220\ \mu M^{-1}\ yr^{-1}$.

OM in the oxic zone. Because biodiffusion is incorporated in the model, this value is now estimated from the analytical solution of the advection–diffusion equation (26) as

$$\bar{C}_{OM} \approx C_{OM}(0) = C^0_{OM} = \frac{2F^0_{OM}}{\rho(1-\phi)\left[w + \sqrt{w^2 + 4D_b k}\right]} \approx \frac{F^0_{OM}}{\rho(1-\phi)\sqrt{D_b k}} \qquad (48)$$

The approximation step on the far right of (48) is valid for large $D_b$, i.e. when biodiffusion dominates the advective transport of OM.

As we assume full degradation of OM and full reoxidation of sulphide, the oxygen flux into the sediment must match the flux of organic carbon, i.e. $F^0_{O_2} \approx F^0_{OM}$. This has the important consequence that the oxygen flux is not dependent on the intensity of bioturbation. This (approximate) theoretical result confirms the simulated oxygen fluxes in Figure 6c, which remain nearly invariant with the biodiffusion coefficient for a given carbon flux. Equally, under the same conditions of full degradation of OM and full reoxidation of sulphide, the oxygen penetration depth is given by expression (44). Again, it is observed

that both transport (here advection *and* bioturbation) and reaction of OM do not influence the oxygen penetration depth. Combining expressions (44) and (48), the total aerobic mineralization and total sulphate reduction can be estimated as

$$\hat{R}^{OR}_{min} \approx \delta_{O_2}\rho(1-\phi)k\bar{C}_{OM} = 2\phi D^s_{O_2} C^0_{O_2} k \frac{1}{\left[w+\sqrt{w^2+4D_b k}\right]} \approx \phi D^s_{O_2} C^0_{O_2}\sqrt{\frac{k}{D_b}} \quad (49)$$

$$\hat{R}^{SR}_{min} \approx F^0_{OM} - 2\phi D^s_{O_2} C^0_{O_2} k \frac{1}{\left[w+\sqrt{w^2+4D_b k}\right]} \approx F^0_{OM} - \phi D^s_{O_2} C^0_{O_2}\sqrt{\frac{k}{D_b}} \quad (50)$$

The fraction of total oxygen consumption due to aerobic mineralization $\beta$ is calculated from (49)–(50) as

$$\beta = \frac{\hat{R}^{OR}_{min}}{\hat{R}^{OR}_{min}+\hat{R}^{SR}_{min}} = \frac{2\phi D^s_{O_2} C^0_{O_2} k}{F^0_{OM}} \frac{1}{\left[w+\sqrt{w^2+4D_b k}\right]} \approx \frac{\phi D^s_{O_2} C^0_{O_2}}{F^0_{OM}}\sqrt{\frac{k}{D_b}} \quad (51)$$

The expressions (49)–(51) form a clear theoretical support for the trends observed in the numerical simulations of Figure 6. Expression (51) predicts that $\beta$ scales with the inverse root of $D_b$ and hence explains the relative decrease of sulphate reduction at the expense of aerobic mineralization with increasing $D_b$ as seen in Figures 6a and 6b. Since $\hat{R}^{SR}_{min} = \hat{R}^{SO}$ due to total sulphide reoxidation, expression (51) also corroborates the relative decrease of aerobic respiration at the expense of sulphide reoxidation in the total oxygen consumption with increasing $D_b$, as seen in Figure 6d. Furthermore, expression (50) confirms the observation that the flux $F^0_{OM}$ at which sulphate reduction starts (i.e. the flux for which $\hat{R}^{SR}_{min} = 0$ decreases with $D_b$, as it scales with the inverse root of $D_b$.

### *(4) Interactions Between Microorganisms/Macroorganisms: Bioirrigation*

Finally, we investigate the response of our ecosystem model to the inclusion of bioirrigation. This macrofaunal transport process is associated with large sedentary benthos, and its description is based on the non-local formulation (5), which states that equal fluid volumes are exchanged between the overlying water column and the porewater at depth (Emerson et al., 1984; Boudreau, 1984; Koretsky et al., 2002). This exchange process will inject oxygen (and possibly sulphate) at depth and at the same time remove sulphide. Figure 7 shows the simulation results for increasing values of the irrigation constant $\alpha$. Some specific trends in rates and fluxes are observed with increasing $\alpha$. (1) The response of the percentages of aerobic mineralization and sulphate reduction in total mineralization (Figures 7a and 7b) and the relative share of aerobic respiration versus sulphide re-oxidation in the total oxygen consumption (Figure 7d) are straightforward. Injection of oxygen and removal of sulphide explain these trends adequately. (2) Figure 7e depicts the importance of bioirrigation relative to diffusion in the total oxygen supply to the sediment. For $\alpha > 1\ yr^{-1}$ a significant part of the total oxygen supply is due to bioirrigation, independent of the organic carbon flux reaching the SWI. (3) The non-monotonic response of the total oxygen flux with increasing values of $F^0_{OM}$ is intriguing and requires closer inspection. As shown by the markings on

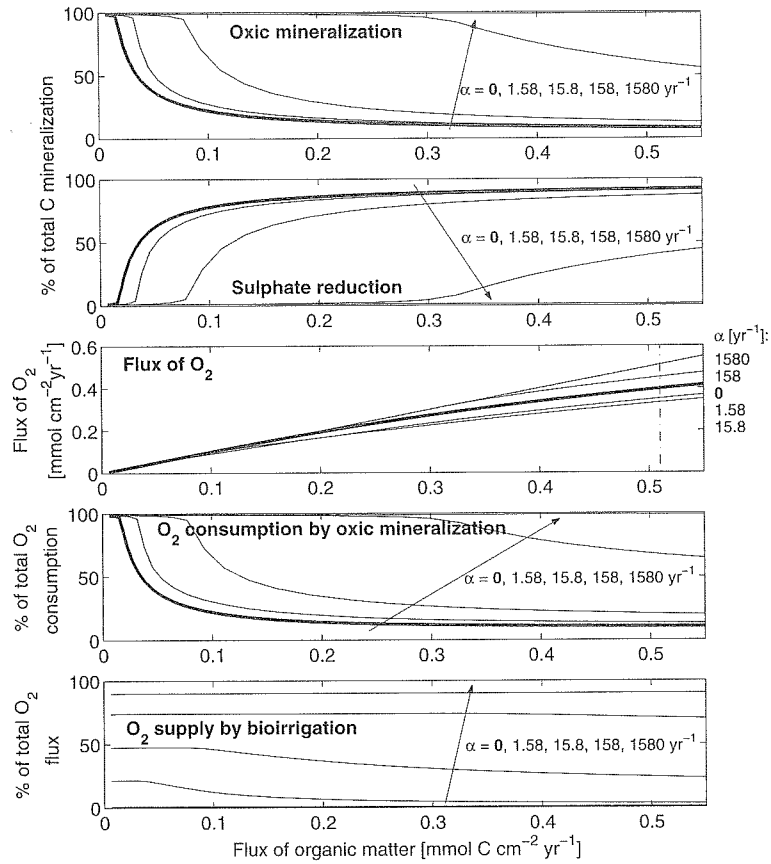


Figure 7. Five-species ecosystem (aerobic respirers + sulphate reducers + sulphide oxidizers + bioturbators + bioirrigators). Dependence of the mineralization pathways, the oxygen flux, the percentage of the oxygen consumption by oxic mineralization, and the oxygen supply by irrigation as a function of the flux of OM. The arrows represent the trend with an increase of the bioirrigation parameter α. Fixed parameter values: $k = 0.1\ yr^{-1}$, $K_{O_2} = 3.1\ \mu M$, $k_{HS^- - O_2} \equiv 220\ \mu M^{-1}\ yr^{-1}$, $D_b = 1\ cm\ yr^{-1}$.

the right hand side of Figure 7c, the total oxygen flux first decreases with increasing α, while past a value of $\alpha > 15.8\ yr^{-1}$ the trend reverses, and the total oxygen flux again increases.

To expose the cause of this non-monotonic response, the depth profiles of all solute species at a specific flux $F^0_{OM} = 0.51\ mmol\ cm^{-2}\ yr^{-1}$ are depicted in Figure 8. One particular feature of the oxygen profile is the oxygenated zone at depth. This is due to the assumption of a constant irrigation with depth and an exponentially decreasing oxygen consumption due to mineralization. The assumption of a constant irrigation rate is not very realistic, however, as macrofaunal activity typically decreases with depth. Accordingly, this accumulation of oxygen at depth may be regarded an artefact due to improper model assumptions. Despite this artefact, the overall trend in the solute inventories with increasing values of α in Figure 7 remains sensible: a steady increase of the total inventory of

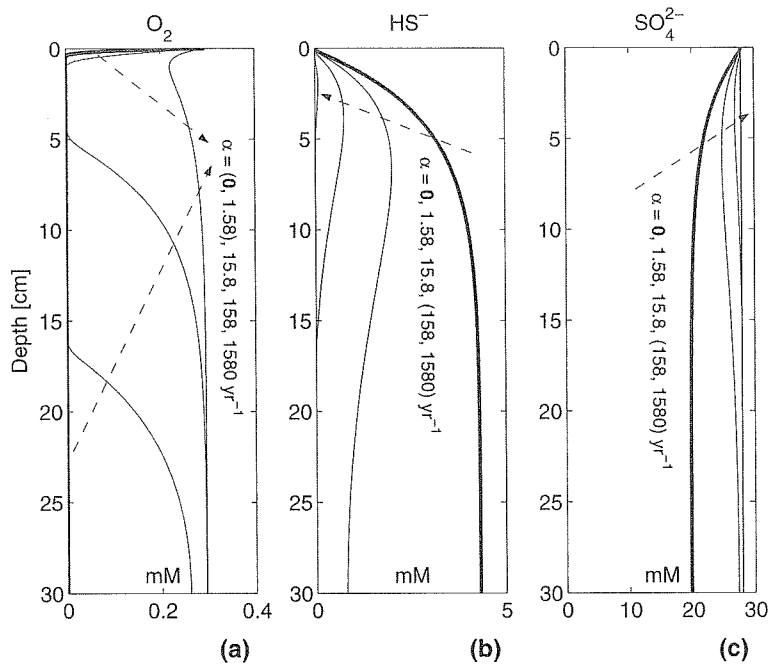


Figure 8. Concentration profiles of solute species corresponding to an OM flux of 0.51 mmol $cm^{-2}$ $yr^{-1}$ (indicated by vertical dashed line in Figure 7c). The parentheses aggregate parameters for which the curves fall together.

oxygen and sulphate, and a decrease of the total inventory of sulphide. This trend is readily explicable: The enhanced supply of oxygen by bioirrigation suppresses the production of sulphide via sulphate reduction.

The bar diagrams of Figure 9 detail the contributions of diffusion and bioirrigation to the total oxygen and sulphide flux. For the oxygen flux, one observes two opposing trends: (1) the diffusive flux decreases monotonically (Figure 9a) as the oxygen penetration depth increases (Figure 8a), and (2) the irrigation flux increases monotonically (Figure 9a). The combined effect is that the total oxygen flux passes through a minimum, as observed in Figures 7c and 9a. In a very similar fashion, the sulphide flux is also subject to two opposing tendencies: (1) The diffusive flux decreases (Figure 9b) because the inventory $HS^-$ is reduced, leading to a less steep gradient near the SWI (Figure 8b), and (2) the irrigation flux first increases due to increasing $\alpha$, but then decreases again because the sulphide in the sediment becomes depleted (Figures 8b and 9b). The overall result shows that the total sulphide flux goes through a maximum, to vanish completely at high values of $\alpha$.

Figure 9b shows a large ventilation effect of sulphide out of the sediment due to bioirrigation. One can question if this model result bears any significance for the actual exchange of sulphide across the SWI. Even in high-carbon-loaded sediments, there is generally little transfer of sulphide to the overlying water column. Moreover, the reaction between sulphide and oxygen is very fast, and energetically favourable for the sulphide oxidizing bacteria involved. Rather, one can question the accuracy of the non-local source/sink expression for bioirrigation that is presently used in 1D reactive-transport

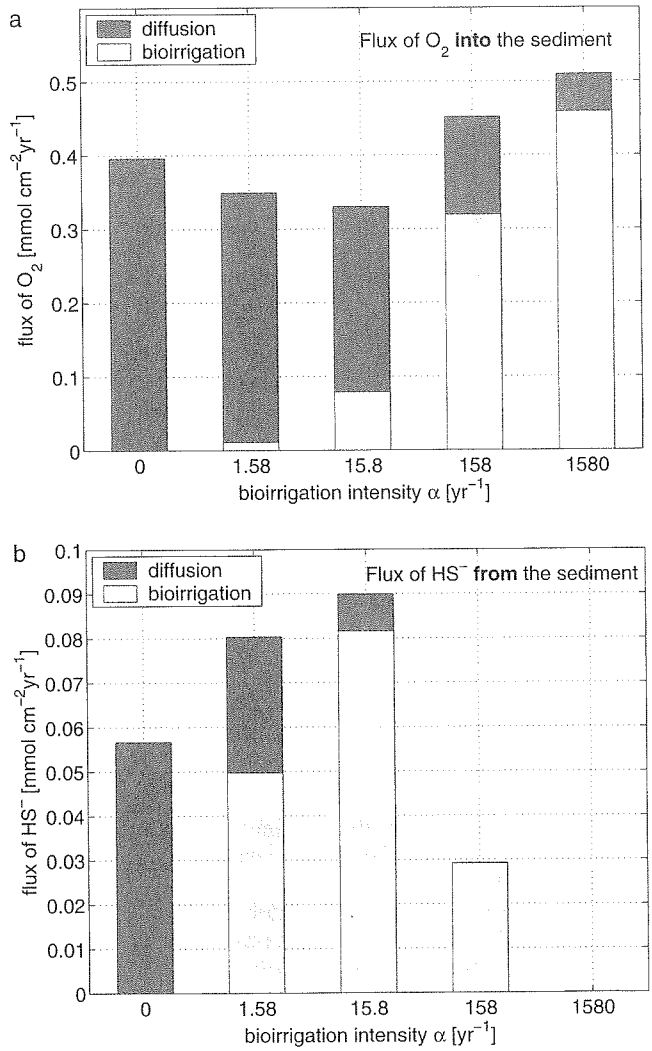


Figure 9. The contributions of diffusion and bioirrigation to the total flux of oxygen across the SWI (above), and the contributions of diffusion and bioirrigation to the total flux of sulphide across the SWI (below). The simulations correspond to the situations depicted in Figures 7 and 8.

models of surface sediments. This 1D-irrigation formalism basically exchanges a sulphide-rich volume of porewater at depth for an identical sulphide-free volume of overlying water. In reality, bioirrigation is a complex 3D process, which is thought to be mainly driven by burrow ventilation and diffusive transfer of solutes across burrow walls. This is more accurately modelled by the 2D tube-irrigation model of Aller (1980), where the sediment is idealized as a collection of identical adjacent cylindrical "burrow territories", and bioirrigation is modelled as radial diffusion of solutes from the burrow

through the burrow wall to the surrounding sediment. Nevertheless, Boudreau (1984) showed that the present 1D-irrigation model can be derived from the Aller (1980) 2D tube-irrigation mechanism by spatial averaging. However, Boudreau (1984) showed that this averaging procedure was only valid given rather strict conditions. The fast reoxidation of sulphide appears to violate these constraints, creating artefacts when applying the 1D model to simulate sulphide bioirrigation. In the 2D model, the sulphide would react with oxygen in the boundary layer near the burrow wall and would not escape the sediment. In the 1D formalism, this sulphide reoxidation is not accounted for, resulting in to the too large sulphide transfer to the water column as predicted in the numerical simulations.

## Conclusion

Opposite to the box-model approach typically used in ecosystem models, a more detailed representation of the sediment is provided by the spatially explicit reactive transport description of diagenetic models. We have shown that diagenetic models can be considered as rudimentary ecosystems models, although diagenetic models are mostly developed for geochemical purposes (Boudreau, 1997). Despite the strong biological abstraction, the activity of macrofauna and the metabolism of certain microbial functional groups are explicitly modelled. This way, diagenetic models have the potential to act as a basic platform to investigate interactions between functional groups. However, to specifically address ecological questions, the biology appears underdeveloped. At present, diagenetic models include only the microbial competition for metabolic resources (OM, terminal electron acceptors) and the effect that macrofauna exerts on this competition via the redistribution of solute and solid reactants. Future extensions could include (1) the feedback of microbial metabolism on macrofaunal activity via the environment (e.g. the inhibition of bioturbation and bioirrigation by sulphide produced in sulphate reduction), (2) the incorporation of biomass dynamics of bacteria (e.g. Talin et al., 2003) and macrofauna, and (3) the inclusion of direct interactions between biological components (grazing, predation, viral lysis). However, this will also require adequate data to validate such process models.

To assess the ecological dimension of present diagenetic models, we have presented a simplified reactive transport model of OM diagenesis, and performed a systematic analysis of the "biological" parameters associated with microbial and macrofaunal functional groups in this model. The (virtual) baseline model included only two bacterial groups: aerobic respirers and sulphate reducers. The additional inclusion of the sulphide reoxidizing bacteria brought in competition for oxygen, and as expected, resulted in a shift from aerobic respiration to sulphate reduction. Further inclusion of bioturbation increased the share of sulphate reduction in mineralization at the expense of aerobic mineralization, the result of a reduced residence time of OM in the oxic zone of the sediment. Finally, the injection of oxygen at depth due to bioirrigation shifted again the mineralization from the anoxic to the oxic pathway. Overall, this sequence of relatively simple diagenetic models illustrated how microbial transformations and macrofaunal transport influence the processing of OM in the sediment.

These dynamics prove at times complex and non-linear, and as a consequence, linear thinking and back-of-the envelope calculations may fall short. Integrated reactive-transport descriptions—such as the one presented here—therefore offer an efficient tool to entangle these complex interactions. However, our simulations also show that one should not trust the output of numerical models blindly. In order to corroborate the results of numerical simulations, we have compared them to (simplified) theoretical results that are based on first-order approximations. The combination of both procedures forms an excellent way

to detect artefacts in the model output, which may originate from different sources. *(1) Invalid model assumptions*. The assumption that the bioirrigation rate remains constant with depth, resulted in an unrealistic accumulation of oxygen at depth. *(2) Invalid process models*. The present 1D non-local irrigation description was shown to be deficient to properly model the fluxes of oxygen and sulphide across the SWI. Note that the constancy of biological transport parameters is a common assumption in present diagenetic models, and the 1D-irrigation description is a widely used process model.

*Acknowledgment.* This study was funded by the EU projects NAME (EVK3-CT-2001-00066) and COSA (EVK3-CT-2002-00076) and supported by a PIONEER grant to Jack Middelburg from the Netherlands Organization for Scientific Research (NWO). We greatly appreciated the constructive remarks of Bernie Boudreau, Dick Van Oevelen, Peter Berg, and an anonymous reviewer. These comments significantly helped to improve the manuscript. This is publication 3361 of the NIOO-KNAW (Netherlands Institute of Ecology).

## References

Aller, R. C., Quantifying Solute Distributions in the Bioturbated Zone of Marine-Sediments by Defining an Average Micro-Environment. *Geochim. Cosmochim. Acta*, 44, 1955-1965, 1980.

Aller, R. C., The effects of macrobenthos on chemical properties of marine sediment and overlying water, in *Animal-sediment relations*, edited by P. L. McCall and M. J. S. Tevesz, pp. 53-102, Plenum, New York, 1982.

Aller, R. C., Transport and Reactions in the Bioirrigated Zone, in *The Benthic Boundary Layer*, edited by B. P. Boudreau and B. B. Jorgensen, pp. 269-301, Oxford University Press, Oxford, 2001.

Aller, R. C. and J. E. Mackin, Preservation of reactive organic matter in marine sediments. *EPSL*, 70, 260-266, 1984.

Barry, D. A., H. Prommer, C. T. Miller, P. Engesgaard, A. Brun, and C. Zheng, Modelling the Fate of Oxidisable Organic Contaminants in Groundwater. *Adv. Water Resour.*, 25, 945-983, 2002.

Bear, J. and Y. Bachmat, *Introduction to Modeling of Transport Phenomena in Porous Media*. pp. 553, Kluwer Academic Publishers, Dordrecht, 1991.

Berg, P., S. Rysgaard, P. Funch, and M. K. Sejr, Effects of Bioturbation on Solutes and Solids in Marine Sediments. *Aquat. Microb. Ecol.*, 26, 81-94, 2001.

Berg, P., S. Rysgaard, and B. Thamdrup, Dynamic Modeling of Early Diagenesis and Nutrient Cycling. A Case Study in an Arctic Marine Sediment. *Am. J. Sci.*, 303, 905-955, 2003.

Berner, R. A., An Idealized Model of Dissolved Sulfate Concentration in Recent Sediments. *Geochim. Cosmochim. Acta*, 28, 1497-1503, 1964.

Berner, R. A., *Early Diagenesis: A Theoretical Approach*. pp. 241, Princeton University Press, Princeton, 1980.

Blackford, J. C., An Analysis of Benthic Biological Dynamics in a North Sea Ecosystem Model. *J. Sea Res.*, 38, 213-230, 1997.

Boudreau, B. P., On the Equivalence of Nonlocal and Radial-Diffusion Models for Porewater Irrigation. *J. Mar. Res.*, 42, 731-735, 1984.

Boudreau, B. P., Mathematics of Tracer Mixing in Sediments: I. Spatially-Dependent, Diffusive Mixing. *Am. J. Sci.*, 286, 161-198, 1986.

Boudreau, B. P., Modeling the Sulfide-Oxygen Reaction and Associated Ph Gradients in Porewaters. *Geochim. Cosmochim. Acta*, 55, 145-159, 1991.

Boudreau, B. P., A Kinetic-Model for Microbic Organic-Matter Decomposition in Marine-Sediments. *Fems Microbiol. Ecol.*, 102, 1-14, 1992.

Boudreau, B. P., A Method-of-Lines Code for Carbon and Nutrient Diagenesis in Aquatic Sediments. *Comput. Geosci.*, 22, 479-496, 1996.

Boudreau, B. P., The Diffusive Tortuosity of Fine-Grained Unlithified Sediments. *Geochim. Cosmochim. Acta*, 60, 3139-3142, 1996.

Boudreau, B. P., *Diagenetic Models and Their Implementation*. pp. 414, Springer, Berlin, 1997.

Boudreau, B. P., Mean Mixed Depth of Sediments: the Wherefore and the Why. *Limnol. Oceanogr.*, 43, 524-526, 1998.

Boudreau, B. P., A Theoretical Investigation of the Organic Carbon-Microbial Biomass Relation in Muddy Sediments. *Aquat. Microb. Ecol.*, 17, 181-189, 1999.

Boudreau, B. P., The Mathematics of Early Diagenesis: From Worms to Waves. *Rev. Geophys.*, 38, 389-416, 2000.

Buisman, C., P. Ijspeert, A. Janssen, and G. Lettinga, Kinetics of Chemical and Biological Sulfide Oxidation in Aqueous-Solutions. Water Res., 24, 667-671, 1990.

Brun, A. and P. Engesgaard, Modelling of Transport and Biogeochemical Processes in Pollution Plumes: Literature Review and Model Development. *J. Hydrol.*, 256, 211-227, 2002.

Cai, W. J. and F. L. Sayles, Oxygen Penetration Depths and Fluxes in Marine Sediments. *Mar. Chem.*, 52, 123-131, 1996.

Chardy, P. and J. C. Dauvin, Carbon Flows in a Subtidal Fine Sand Community From the Western English-Channel - a Simulation Analysis. *Mar. Ecol.-Prog. Ser.*, 81, 147-161, 1992.

Crank, J., *The Mathematics of Diffusion*. Oxford University Press, Oxford, 1975.

Dauwe, B., J. J. Middelburg, and P. M. J. Herman, Effect of Oxygen on the Degradability of Organic Matter in Subtidal and Intertidal Sediments of the North Sea Area. *Mar. Ecol.-Prog. Ser.*, 215, 13-22, 2001.

Dhakar, S. P. and D. J. Burdige, Coupled, Non-Linear, Steady State Model for Early Diagenetic Processes in Pelagic Sediments. *Am. J. Sci.*, 296, 296-330, 1996.

Ebenhoh, W., C. Kohlmeier, and P. J. Radford, The Benthic Biological Submodel in the European-Regional-Seas-Ecosystem-Model. *Neth. J. Sea Res.*, 33, 423-452, 1995.

Emerson, S., Organic carbon preservation in marine sediments, in *The Carbon Cycle and Atmospheric CO2: Natural Variations Archean to Present*, edited by E. T. Sundquist and W. S. Broecker, pp. 78-87, AGU, Washington, D.C., 1985.

Emerson, S., R. Jahnke, and D. Heggie, Sediment-Water Exchange in Shallow-Water Estuarine Sediments. *J. Mar. Res.*, 42, 709-730, 1984.

FEMLAB Chemical Engineering Module, 2002, COMSOL AB, Tegnergatan 23, SE-111 40 Stockholm, Sweden (http://www.femlab.com).

Fenchel, T., G. M. King, and T. H. Blackburn, *Bacterial Biogeochemistry*. pp. 307, Academic Press, San Diego, CA, 1998.

Giles, M. R., *Diagenesis: A Quantitative Perspective*. Norwell, Massachusetts, 1997.

Goldberg, E. D. and M. Koide, Geochronological studies of deep-sea sediments by the Io/Th method. *Geochim. Cosmochim. Acta*, 26, 417-450, 1962.

Guinasso, N. L. and D. R. Schink, Quantitative Estimates of Biological Mixing Rates in Abyssal Sediments. *J. Geophys. Res.-Ocean. Atmos.*, 80, 3032-3043, 1975.

Heip, C. H. R., N. K. Goosen, P. M. J. Herman, J. Kromkamp, J. J. Middelburg, and K. Soetaert, Production and Consumption of Biological Particles in Temperate Tidal Estuaries. *Oceanography and Marine Biology - an Annual Review*, 33, 1-149. 1995.

Hensen, C., H. Landenberger, M. Zabel, J. K. Gundersen, R. N. Glud, and H. D. Schulz, Simulation of Early Diagenetic Processes in Continental Slope Sediments Off Southwest Africa: the Computer Model COTAM Tested. *Mar. Geol.*, 144, 191-210, 1997.

Herman, P. M. J., J. J. Middelburg, J. Van De Koppel, and C. H. R. Heip, Ecology of Estuarine Macrobenthos. *Adv. Ecol. Res.*, 29, 195-240, 1999.

Huettel, M., W. Ziebis, S. Forster, and G. W. Luther, Advective transport affecting metal and nutrient distributions and interfacial fluxes in permeable sediments. *Geochim. Cosmochim. Acta*, 62, 613-631, 1998.

Hunter, K. S., Y. F. Wang, and P. Van Cappellen, Kinetic Modeling of Microbially-Driven Redox Chemistry of Subsurface Environments: Coupling Transport, Microbial Metabolism and Geochemistry. *J. Hydrol.*, 209, 53-80, 1998.

Huyakorn, P. S. and G.F. Pinder, *Computational Methods in subsurface flow*. Academic Press, San Diego, CA, 1983.

Jorgensen, B. B., Mineralization of Organic Matter in the Sea Bed - the Role of Sulphate Reduction. *Nature*, 296, 643-645, 1982.

Koretsky, C. M., C. Meile, and P. Van Cappellen, Quantifying Bioirrigation Using Ecological Parameters: a Stochastic Approach. *Geochem. Trans.*, 3, 17-30, 2002.

Lichtner, P. C., Continuum model for simultaneous chemical reactions and mass transport in hydrothermal systems. *Geochim. Cosmochim. Acta*, 49, 779-800, 1985.

Meysman, F. J. R., *Modelling the Influence of Ecological Interactions on Reactive Transport Processes in Sediments*. PhD Dissertation, pp. 213, Ghent University, 2001.

Meysman, F. J. R., B. P. Boudreau, and J. J. Middelburg, Relations Between Local, Nonlocal, Discrete and Continuous Models of Bioturbation. *J. Mar. Res.*, 61, 391-410, 2003.

Meysman, F. J. R., J. J. Middelburg, P. M. J. Herman, and C. H. R. Heip, Reactive Transport in Surface Sediments. II. Media: an Object-Oriented Problem-Solving Environment for Early Diagenesis. *Comput. Geosci.*, 29, 301-318, 2003.

Millero, F. J., S. Hubinger, M. Fernandez, and S. Garnett, Oxidation of $H_2S$ in seawater as a function of temperature, pH, and ionic strength. *Environ. Sci. Technol.*, 21, 439-443, 1987.

Moore, J. C., E. L. Berlow, D. C. Coleman, P. C. De Ruiter, Q. Dong, A. Hastings, N. C. Johnson, K. S. Mccann, K. Melville, P. J. Morin, K. Nadelhoffer, A. D. Rosemond, D. M. Post, J. L. Sabo, K. M. Scow, M. J. Vanni, and D. H. Wall, Detritus, Trophic Dynamics and Biodiversity. *Ecol. Lett.*, 7, 584-600, 2004.

Rhoads, D. C., Organism-sediment relations on the muddy sea floor. *Oceanogr. Mar. Biol.*, 12, 263-300, 1974.

Rittmann, B. E. and J. M. VanBriesen, Microbial Processes in Reactive Modeling, in *Reactive Transport in Porous Media*, edited by P. C. Lichtner, C. C. Steefel, and E. H. Oelkers, pp. 311-334, The Mineralogical Society of America, Washington, 1996.

Salvage, K. M. and G. T. Yeh, Development and Application of a Numerical Model of Kinetic and Equilibrium Microbiological and Geochemical Reactions (Biokemod). *J. Hydrol.*, 209, 27-52, 1998.

Soetaert, K., P. M. J. Herman, and J. J. Middelburg, A Model of Early Diagenetic Processes From the Shelf to Abyssal Depths. *Geochim. Cosmochim. Acta*, 60, 1019-1040, 1996a.

Soetaert, K., P. M. J. Herman, and J. J. Middelburg, Dynamic Response of Deep-Sea Sediments to Seasonal Variations: a Model. *Limnol. Oceanogr.*, 41, 1651-1668, 1996b.

Soetaert, K., J. Middelburg, J. Wijsman, P. Herman, C. Heip, Ocean Marin Diagenetic Processes and Models, in *Ocean Margin Systems*, edited by G. Wefer, D. Billett, D. Hebbeln, B. B. Jorgensen, M. Schluter, and T. Van Weering, pp. 155-177, Springer-Verlag, Berlin Heidelberg, 2002.

Steefel, C. I. and K. T. B. MacQuarrie, Approaches to Modeling of Reactive Transport in Porous Media, in *Reactive Transport in Porous Media*, edited by P. C. Lichtner, C. C. Steefel, E. H. Oelkers, pp. 83-129, The Mineralogical Society of America, Washington, 1996.

Talin, F., C. Tolla, C. Rabouille, and J. C. Poggiale, Relations between Bacterial Biomass and Carbon Cycle in Marine Sediments: an Early Diagenetic Model. *Acta Biotheoretica*, 51, 295-315, 2003.

Tan, Y. and W. J. Bond, Modeling subsurface transport of microorganisms, in *Environmental Hydrology*, edited by V. P. Singh, pp. 321-355, Kluwer Academic Publishers, Dordrecht, 1995.

Van Cappellen, P. and J. F. Gaillard, Biogeochemical Dynamics in Aquatic Sediments, in *Reactive Transport in Porous Media*, edited by P. C. Lichtner, C. C. Steefel, and E. H. Oelkers, pp. 335-376, The Mineralogical Society of America, Washington, 1996.

Van Cappellen, P., J.-F. Gaillard, and C. Rabouille, Biogeochemical transformations in sediments: kinetic models of early diagenesis, in *Interactions of C, N, P and S Biogeochemical Cycles and Global Change*, edited by R. Wollast, F. T. Mackenzie, and L. Chou, pp. 401-445, Springer-Verlag, New York, 1993.

Van Cappellen, P. and Y. F. Wang, Metal Cycling in Surface Sediments: Modeling the Interplay of Transport and Reaction, in *Metal Contaminated Sediments*, edited by H. E. Allen, pp. 21-64, Ann Arbor Press, Chelsea, MI, 1995.

Wang, Y. F. and H. W. Papenguth, Kinetic Modeling of Microbially-Driven Redox Chemistry of Radionuclides in Subsurface Environments: Coupling Transport, Microbial Metabolism and Geochemistry. *J. Contam. Hydrol.*, 47, 297-309, 2001.

Wijsman, J. W. M., P. M. J. Herman, J. J. Middelburg, and K. Soetaert, A Model for Early Diagenetic Processes in Sediments of the Continental Shelf of the Black Sea. *Estuar. Coast. Shelf Sci.*, 54, 403-421, 2002.